CHALMERS

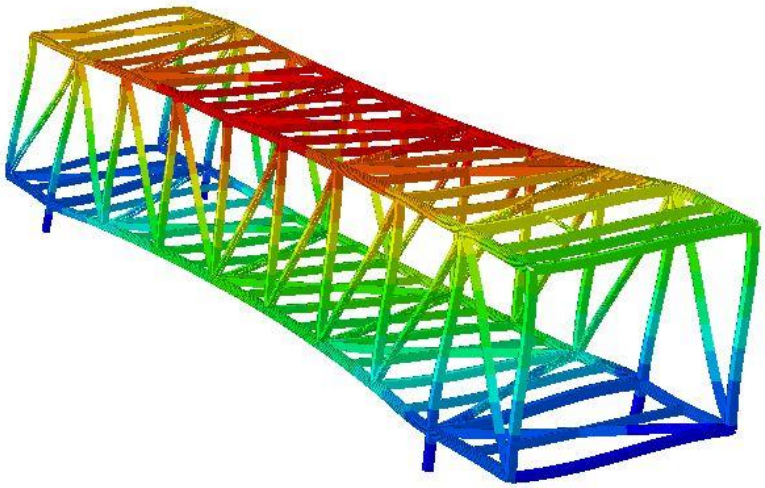

Dynamic response of pipe rack steel structures to explosion loads

Master's Thesis within the Structural Engineering and Building Technology programme

ANTON STADE AARØNÆS, HANNA NILSSON

Department of Civil and Environmental Engineering
Division of Structural Engineering
CHALMERS UNIVERSITY OF TECHNOLOGY
Göteborg, Sweden 2014
Master's Thesis 2014:117

MASTER'S THESIS

Dynamic response of pipe rack steel structures to explosion loads

Master's Thesis within the Structural Engineering and Building Technology programme

ANTON STADE AARØNÆS, HANNA NILSSON

SUPERVISOR:

Reza Haghani Dogaheh

EXAMINER

Reza Haghani Dogaheh

Department of Civil and Environmental Engineering
Division of Structural Engineering
CHALMERS UNIVERSITY OF TECHNOLOGY
Göteborg, Sweden 2014

Master's Thesis 2014:117

Dynamic response of pipe rack steel structures to explosion loads
Master's Thesis within the *Structural Engineering and Building Technology* programme
ANTON STADE AARØNÆS, HANNA NILSSON

Department of Civil and Environmental Engineering
Division of Structural Engineering
Chalmers University of Technology
SE-412 96 Göteborg
Sweden
Telephone: + 46 (0)31-772 1000

Cover:
Deformed pipe rack steel structure exposed to explosion loading. Modelled in Abaqus/CAE with enhanced deflections for illustrative purposes.

Chalmers Reproservice
Göteborg, Sweden 2014
Master's Thesis 2014:117

Dynamic response of pipe rack steel structures to explosion loads
Master's Thesis in the *Structural Engineering and Building Technology* programme
ANTON STADE AARØNÆS, HANNA NILSSON
Department of Civil and Environmental Engineering
Division of Structural Engineering
Chalmers University of Technology

ABSTRACT

When performing dynamic explosion analyses on steel pipe racks, a common simplified method is to apply the static load multiplied by a fixed dynamic amplification factor (DAF). By adapting this amplification, a static analysis is sufficient to account for both static and dynamic behaviour in design. Consequently, all structures independent of stiffness and mass properties are provided with the same degree of dynamic amplification which can produce a high level of conservatism in their design.

The objective of this thesis is to gain a better understanding of the dynamic behaviour of pipe rack steel structures subjected to explosion loading. By achieving this, the aim is to provide structural engineers with knowledge leading to a more accurate design in future projects.

To accomplish this, finite element analyses of three pipe racks have been performed and their respective DAFs have been calculated. The results show that DAFs vary between the structures, which indicate that the dynamic behaviour depends on one or several parameters. In addition, the results indicate that the magnitude of the DAF is dependent on what the selected inputs to calculate the DAF are. However, as no obvious affinity between the parameters of the structures and the dynamic amplification is observed, a parametric study was required to increase the understanding of how different parameters affect the DAF. The results from the parametric study show the same variation of the DAF as in the analyses of the first three pipe racks. The results even reveal DAFs higher than the DAFs currently used in design procedures. Moreover, the results show that the mass distribution has a significant influence on the dynamic behaviour. In addition, the results indicate that the DAF currently utilized in design is non-conservative. However, the rather large scatter of the results implies that further studies are desired.

Key words: pipe rack, dynamic behaviour, explosion, DAF, FEA,
pipe mass distribution, base shear, overturning moment

Dynamisk respons av fackverksstrukturer i stål på grund av explosionslaster
Examensarbete inom masterprogrammet *Konstruktions- och byggteknik*
ANTON STADE AARØNÆS, HANNA NILSSON
Institutionen för Bygg- och miljöteknik
Avdelningen för Konstruktionsteknik
Chalmers tekniska högskola

SAMMANFATTNING

Vid dynamisk analys av fackverk i stål tillämpas vanligen en förenklad metod. Den innebär att en statisk last multiplicerad med en dynamisk amplifikationsfaktor (DAF), där DAF representerar det dynamiska beteendet hos strukturen. Genom att applicera denna förenklade metod antas en statisk analys vara tillräcklig för att ta hänsyn till både statiskt och dynamiskt beteende. Konsekvensen blir dock att alla strukturer, oberoende av styvhet och massa, konstrueras med samma dynamiska amplifikation. Detta leder i sin tur till konservativa konstruktioner.

Målet med den här avhandlingen är att skapa bättre förståelse gällande det dynamiska beteendet hos fackverk i stål som utsätts för explosionslaster. Förhoppningen är att bistå konstruktörer med kunskap som kan leda till mer verklighetsnära konstruktioner i framtida liknande projekt. För att uppnå detta har först tre fackverksstrukturer analyserats. Resultaten visar att DAF varierar mellan strukturerna vilket tyder på att det dynamiska beteendet beror av en eller flera faktorer. I tillägg visar resultaten att omfattningen av DAF beror av vilket värde den är baserad på. Likväl observeras ingen tendens mellan faktorerna som värderats. En parameterstudie var därför nödvändig för att utvärdera hur olika faktorer påverkar DAF. Resultaten från den parametriska studien visar samma variationer av DAF som i den första studien. Ett av resultaten avslöjar även DAF högre än idag generellt tillämpade DAF. I tillägg influerar tyngdpunktens läge signifikant det dynamiska beteendet.

En slutsats kan dras att tyngdpunktens läge är en väsentlig faktor att ta hänsyn till vid konstruktion av fackverk i stål som utsätts för explosionslaster. I tillägg indikerar resultaten att den nuvarande tillämpade DAF är icke-konservativa. En stor spridning av resultaten finns dock och vidare studier är därför önskvärda.

Nyckelord: fackverk, dynamiskt beteende, explosion, DAF, FEA, massdistribution, basskjuvning, lyftmoment

Contents

Preface

In this study, the dynamic behaviour of pipe rack steel structures due to explosion loads has been studied. The study has been carried out from January to May 2014. The master's thesis has been written for the Department of Civil and Environmental Engineering at Chalmers University of Technology (Chalmers) in collaboration with the Structural Department at Aker Solutions (AKSO) in Oslo as part of the Nyhamna Expansion Project (NYX).

Supervisor for the master's thesis project has been Reza Haghani Saeed (Assistant Professor) from Chalmers and Nicolas Neumann (Structural Discipline Lead) from AKSO. The analyses have been performed at Chalmers and at AKSO. We would like to thank both our supervisors together with the rest of the structural team at NYX for their interest in our work, help and sharing of knowledge.

Oslo June 2014

Anton Stade Aarønæs and Hanna Nilsson

Notations

Roman upper case letters

A	Projected area
C_D	Drag coefficient
F	External force
F_{blast}	Blast point load
F_{drag}	Drag force
L	Structural length
M	Induced moment
R_H, R_V	Support reactions
Re	Reinolds number
R^2	Coefficient of determination
T	Eigen period
V_δ	Error terms coefficient of variation
Q_d	Design load

Roman lower case letters

b	Height
c	Distance between vertical RHSs
e	Eccentricity
f	Eigen frequency
g	Gravity constant
k	Stiffness
l	Length between pipe supports
m	Mass
s	Width
t_d	Blast load duration
u	Flow velocity
v	Blast velocity
x	Displacement

Greek upper case letters

Δt	Required time for blast to travel from front to back frame
ΔPd	Drag peak pressure

Greek lower case letters

α	Spacing ratio
β	Aerodynamic solidity ratio
δ_{static}	Static deflection
$\delta_{dynamic}$	Dynamic deflection
ε	Strain
η	Shielding factor
ρ	Density
υ	Poisson’s ratio

List of abbreviations

AGSM	Approximate Global Mesh Size
AKSO	Aker Solutions
AR	Aspect Ratio
BC	Boundary Condition
BS	Base Shear
CAE	Complete Abaqus Environment
CFD	Computational Fluid Dynamics
CoM	Centre of Mass
CPU	Central Processing Unit
DAF	Dynamic Amplification Factor
DAL Spec.	Design Accidental Load Specification
FEA	Finite Element Analysis
MDOF	Multiple Degrees of Freedom
NYX	Nyhamna Expansion Project
OT	Overturning Moment
RHS	Rectangular Hollow Section
RF	Resulting Force
SDOF	Single Degree of Freedom
TWUL	Total Weight per Unit Length

1 Introduction

This thesis with the title Dynamic response of pipe rack steel structures to explosion loads is written by Hanna Nilsson and Anton Stade Aarønæs from Chalmers University of Technology in cooporation with Aker Solutions (AKSO). The thesis is part of the Nyhamna Expansion Project (NYX) which is the expansion of Shell's existing onshore gas facilities situated on the Norwegian west coast. As an introduction to the study, the background and objectives of the thesis are presented in the following chapter.

1.1 Background

As mentioned above, this master's thesis is part of the expansion of the onshore gas facility at Nyhamna. From Figure 1-1 an overview of the plant is depicted with the new buildings and structures highlighted in green.

Figure 1-1 Overview of the Nyhamna plant with new buildings and structures.

Nyhamna is the location and name of the gas facility where gas from the second largest gas field in Norway (Ormen Lange) is processed and compressed before it is exported through one of the world's longest subsea pipelines (Langeled) to Easington in south England (Shell, 2014). In order to distribute the gas between the different process areas at the facility, a web of pipes and pipe supporting structures such as pipe racks are required. In Figure 1-2 on the next page, the letdown area (gas arrival/departure area) and booster compression area are presented. The figure visualizes how the pipes are routed between the two areas through a pipe rack spanning one of the facility roads (red circle). A detailed sketch of the pipe rack outlined by a red circle visualizes the truss shaped pipe rack with pipes running longitudinally on two levels and supported on a foundation of concrete columns. More pipe rack features and the reason for the chosen structures to be analysed are presented in Chapter 4.

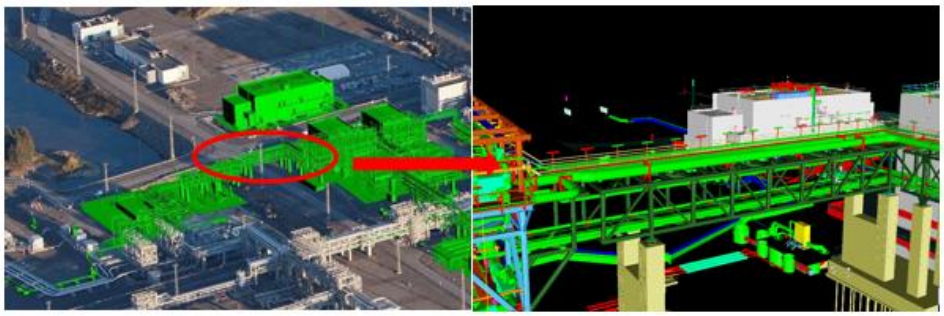

Figure 1-2 Pipe rack between letdown and booster compression area at Nyhamna.

In NYX the governing load for a majority of the structures is explosion loading. In traditional design, the pressure load caused by an explosion is considered as a quasi-static pressure load. A quasi-static load is varying over time but it is considered to be "slow" enough to neglect time and inertial mass effects (Yavari, 2010), i.e. the load can be represented as a static load. When the quasi-static pressure load distribution on the structure is determined, the dynamic response is taken into consideration by multiplying the static load by a dynamic amplification factor (DAF). There is a variation in how DAF is referred to in literature but it will consistently be denoted as DAF in this report.

The dynamic response is influenced by a range of parameters such as stiffness, geometry and load duration. In design, DAF is determined by calculating the Eigen period (T) as 1 through the Eigen frequency of the structure. The duration of the blast (t_d) is divided by the Eigen period to obtain a DAF-curve as depicted in Figure 1-3, which is based on a single-degree-of-freedom (SDOF) system. However, at NYX a simplified method is adapted where the static loads are multiplied by a fixed DAF to account for the dynamic amplification. There is more than one reason to choose the simplified method. Firstly, the calculations become simplified as no determination of the Eigen period is required. Secondly, as the duration of the blast is a probabilistic value, the simplified method is a conservative assumption independent of the blast duration.

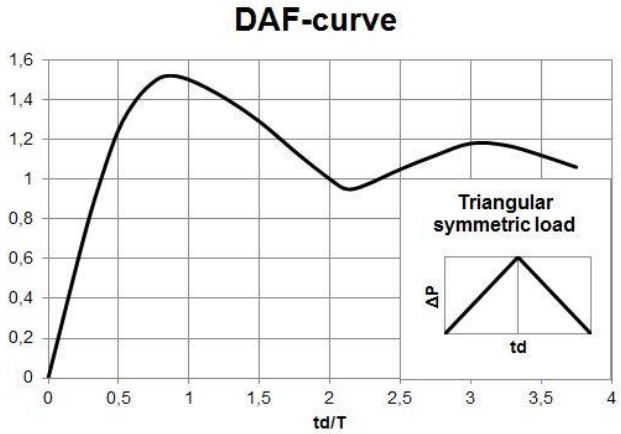

Figure 1-3 Maximum dynamic response of an elastic SDOF-system (undamped) subjected to a triangular load pulse (Biggs, 1964).

It is in the interest of AKSO to give their structural engineers a better tool to determine more realistic DAFs leading to a less conservative design. To realize this, more knowledge on the dynamic behaviour due to explosion loads is required.

1.2 Objective

The aim of this thesis is to increase understanding of the dynamic behaviour of pipe rack steel structures exposed to explosion loads by studying how the structural response is influenced by a set of parameters associated with loading and geometrical configurations. By accomplishing this, the intention is to adapt this knowledge to determine dynamic amplification factors with higher accuracy for similar structures in future projects.

1.3 Limitations

To make the work process efficient and to maintain focus on the objective a number of limitations are established. The choice of structures is limited to onshore steel pipe racks in NYX. They are chosen so that the results and conclusions of the thesis can be applicable to future projects. Furthermore, only structures exposed to near-field explosions are investigated as they are the most common in NYX. In order to evaluate how explosion loads are interacting with the pipe rack structures, computational fluid dynamics (CFD) are performed. The focus in this report is however kept on the behaviour of the structure and not on the details of the interaction between load and structure, and therefore CFD are not performed. The loads utilized in the analyses are calculated based on input from project specific documents from NYX together with recommended calculation practices from Det Norske Veritas AS (DNV).

Pipe supports are designed to be sturdy enough to safely secure their supported pipes in the event of an explosion. If a pipe were to be released during an explosion it could impact with other parts of the structure; this would produce an incalculable series of accidental load cases for the pipe rack.

Damping of the structures is neglected for three reasons. Firstly, damping has minimal effect on the fundamental response peak (Yandzio & Gough, 1999). Moreover, the curve in Figure 1-3 is based on an undamped system and since the results from this study are compared to this figure, damping is not taken into consideration in analysis. Finally, as the damping acts to reduce the dynamic deflection, excluding damping is more conservative.

1.4 Questions at issue

To further state the objective of the thesis, attempt is made to find answers to the following questions.

1) Can the DAF be decreased below its maximum value of 1.5 by tuning certain parameters?
2) Is the DAF-curve from Biggs (ref. Figure 1-3) which is based on a SDOF-system, representative for MDOF-systems?

To find answers to these questions, a study will be performed to examine how the following parameters influence the DAF: geometry of structure, structural stiffness, Eigen period, shielding and turbulence.

2 Theory

It is important to understand the behaviour of an explosion and the way it evolves in time and space to fully understand what happens when the pressure wave from an explosion reaches a structure. This chapter gives a general introduction to structural dynamics and explosion loading and will provide the reader with useful knowledge to understand the content of the study.

2.1 Static and dynamic applications

The application of structural dynamics is different in aerospace engineering, civil engineering, engineering mechanics, and mechanical engineering, although the principles and solution techniques are the same (Craig, 2006). In the following sections the basis of structural dynamics including the difference between static and dynamic loads and dynamic amplification is explained.

2.1.1 SDOF- and MDOF-systems

Structures are expressed as systems of degrees-of-freedom, i.e. the number of independent motions that can take place. A continuous structure has an infinite number of degrees of freedom, i.e. multiple degrees of freedom (MDOF). But to choose an appropriate mathematical model of the structure, a reduction in the number of degrees has to be made (Paz, 1987). The reduction can in some cases be made down to a SDOF. A SDOF-system can for example be expressed as a spring-mass system as depictured in Figure 2-1. The mass of the structure is represented by one lumped mass, *m*, and the stiffness by one spring with stiffness, *k*. The structure is exposed to a force, *F*, and the movement of the mass is expressed by a displacement, *x*, resulting in a complete SDOF-system.

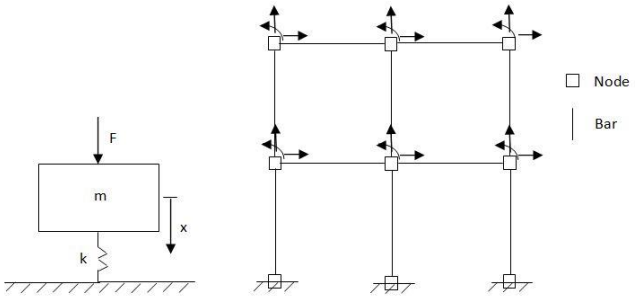

Figure 2-1 A SDOF- system (left) and a MDOF-system (right).

A MDOF-system however, is represented by a number of displacements. The right system in Figure 2-1 illustrates a frame with 18 degrees-of-freedom. The displacements can take place independent of each other. Each bar between the nodes can have individual stiffness and a mass which contribute to the displacement of the nodes when the frame is exposed to forces. The frame could also be expressed as a SDOF-system where all the masses of the bars and all their stiffness are summed up to a global mass and stiffness represented by *m* and *k* as in Figure 2-1. The difference is that when the frame is represented by a SDOF-system the displacement is only expressed as a uniform displacement where the whole structure moves as a lumped mass. The representation of a MDOF-system is closer to the real behaviour of the frame where different parts of the structure moves with different magnitudes.

2.1.2 Static and dynamic loads

The difference between a static and a dynamic analysis is related to how the loads are applied. In a static analysis the loads are static, i.e. time independent, while a dynamic load changes over time. A static load is applied with constant amplitude while the dynamic load can be built up to reach its highest value and subsequently decrease, e.g. a load expressed as a symmetric triangular pulse (ref. Figure 1-3). An example of a dynamic load is the vibrations from machinery on a concrete foundation, while an example of a static load is snow lying still on top of a roof. A load can also be quasi-static which means that it is time-dependent but changes slowly over time so that the time-dependency is negligible and the load can therefore be expressed as a static load.

2.1.2.1 Dynamic amplification factor (DAF)

To represent the dynamic behaviour of a system without performing a dynamic analysis, charts of the maximum response can be used (Biggs, 1964). Figure 1-3 in the introduction chapter illustrates the maximum response of a SDOF-system subjected to a symmetric triangular load pulse. By calculating the Eigen period (T) of the structure and assuming a blast duration (t_d), the DAF can be obtained from the figure.

The DAF is conventionally defined as the ratio between the dynamic deflection at any time to the deflection which would have resulted from the static application of the load as defined in Equation 2.1 (Biggs, 1964). The deflection can be substituted by other parameters, e.g. base shear, overturning moment etc.

$$DAF = \frac{\delta_{dynamic}}{\delta_{static}} \tag{2.1}$$

To analyse the dynamic behaviour of a MDOF-system, finite element analysis (FEA) software such as Abaqus/CAE is strongly recommended to be used instead of numerical solutions by hand. However, performing FEA is both time consuming and expensive with regard to working hours and software licenses respectively.

2.1.3 Analysing structures

Analyses are performed on both existing structures and structures not yet erected. The analytical process when studying the static and the dynamic behaviour is the same independent of the type of structure. When analysing a structure the interesting outputs are often the displacements, stresses, reaction forces and Eigen frequencies. The Eigen frequency is the vibration of the structure when only self-weight and (if relevant) additional inertia masses from equipment acting on the structure. Equation 2.2 is used to calculate the Eigen frequency where k represents the stiffness and m the mass of the system.

$$f = \sqrt{\frac{k}{m}} \tag{2.2}$$

After an analysis is performed, the outputs are compared to given criteria and if they are not fulfilled the structure has to be strengthened or redesigned.

2.2 Introduction to explosion loading

Explosions in chemical facilities such as onshore and offshore petroleum plants are rare events but will nevertheless have vast consequences (Mannan, 2014). It is of great importance for the structural engineer responsible for the design to understand how the explosions behave and in what way it will affect the structures. This chapter is an introduction to explosion loading where the aim is to give the reader an explanation of the behaviour of explosions and what their origins are.

2.2.1 Definition of an explosion

An explosion is an event leading to a rapid increase in pressure and is caused by one or a combination of the following events (Bjerketvedt, et al., 1990):

- nuclear reactions
- loss of containment in high pressure vessels
- explosives
- metal water vapour explosions
- run-a-way reactions
- combustion of dust
- mist of gas (including vapour) in air or in other oxidisers.

This report will only examine chemical explosions as a result of flammable gas, referred to as gas explosions. Such explosions can be derived into two modes: deflagration and detonation (Mannan, 2014). The most common type is deflagration which is defined as the combustion wave propagation at a velocity below the speed of sound i.e. subsonic speed (Bjerketvedt, et al., 1990). The flame speed in a deflagration mode ranges from 1-1000 m/s while the pressure varies between a few mbar to several bar. For near-field explosions the explosions are of the deflagration mode. Since the majority of the structures in NYX are designed for near-field explosions, detonation explosions will not be given further attention. The difference between near-field and far-field explosions will however be explained in detail in the next section.

In addition to a division between the wave propagation velocity, gas explosions are also categorized depending on the environment in which the explosion takes place. There are three main categories; confined gas explosions, partly confined gas explosions and unconfined gas explosions, which by their labels are distinguished by the containment of the explosion environment.

2.2.2 Blast waves

In the case of an explosion there is a sudden release of energy to the atmosphere which will result in a transient pressure also known as a blast wave (ASCE, 2010). Blast waves are distinguished by three categories as depicted in Figure 2-2.

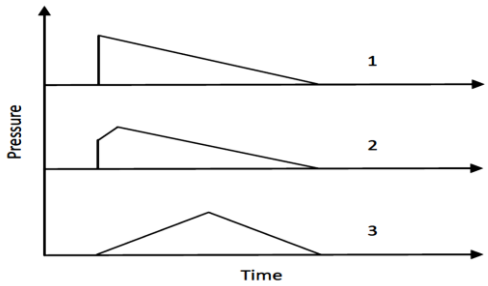

Figure 2-2 Blast waves category 1, 2 and 3.

1. A shock wave[1] followed by a rarefaction wave[2].
2. A shock wave followed by a sonic compression wave and a rarefaction wave.
3. A sonic compression wave and a rarefaction wave (Bjerketvedt, et al., 1990).

The type of blast wave depends on how and when the energy is released in the explosion, as well as the distance from the explosion area (Bjerketvedt, et al., 1990). Category 1 is typical for strong explosions while weaker explosions initially are in category 3, even though the blast wave may end up as category 1 when it propagates away from the explosion. Blast waves from gas explosions are divided into close-in range (near-field), mid-distance and far-field blast waves depending on their peak pressures and the distance from the explosion epicentre. Far field blast waves take the form of curve 1 in Figure 2-2 and near field blast waves take the form of curve 3. The definition of near-field, mid-distance, and far-field blast waves is presented in Table 2-1.

Table 2-1 Classification of near-field, mid-distance and far-field blast waves (Bjerketvedt, et al., 1990).

Classification	Peak overpressure[3]
Near-field	> 0.69 bar
Mid-distance	0.034-0.69 bar
Far-field	< 0.034 bar

[1] A large compressive wave (such as a seismic wave or sonic boom) that is caused by a shock to the medium through which the wave travels (Atkins & Escudier, 2013).
[2] A progressive wave or wave front that causes expansion of the medium through which it propagates (Atkins & Escudier, 2013).
[3] Pressure greater than the hydrostatic pressure (Allaby, 2013).

2.3 Interaction between blast and structure

High explosion pressures in process plants can be generated by a deflagration in congested and confined areas such as inside buildings and pipe bridges, in areas where pipes and equipment are densely packed or in tunnels and culverts (Prud'homme, et al., 2013). When evaluating the consequences of deflagrations, peak pressure, rise time, the duration of the pressure pulse and the impulse should be considered. If a strong gas explosion occurs inside a process area or in a compartment, the surrounding area will be subjected to a blast wave with magnitude depending on:

- the pressure and duration of the explosion
- the distance between the explosion and the structure.

2.3.1 Side-on pressure and reflected pressure

The side-on pressure is the pressure measured perpendicular to the direction of the blast wave direction (Bjerketvedt, et al., 1990). When the blast wave impacts a structure, all flow behind the front is stopped which will result in a reflecting pressure that is considerably greater than the side-on pressure (Baker, et al., 1983). Figure 2-3 illustrates a blast wave propagating towards a solid structure where the shock front is reflected when the blast wave hits the front face.

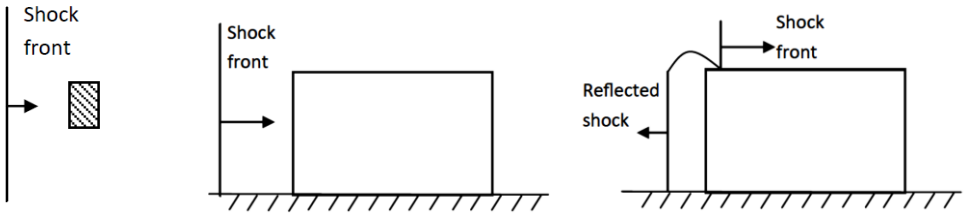

Figure 2-3 A shock front moves towards a small (left) and a larger (right) object and is reflected as it hits the wall facing the direction of the blast wave.

The directions of the side-on pressure and the reflected pressure are illustrated in Figure 2-4, where the reflected pressure is directed in the propagation direction of the blast wave.

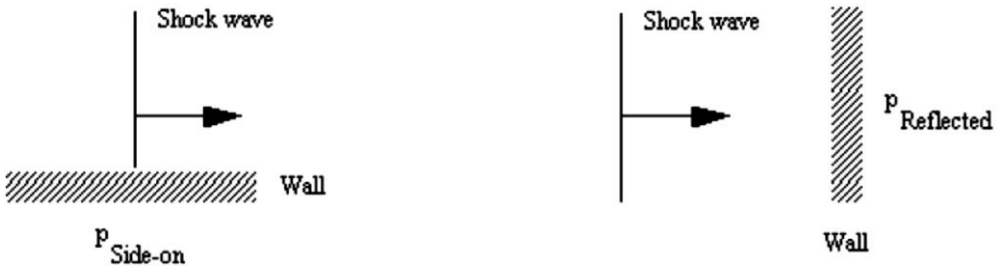

Figure 2-4 Side-on pressure and reflected pressure (Bjerketvedt, et al., 1990).

For objects with small dimensions as the one on the left in Figure 2-3, the shock front moves so quickly that reflection does not have to be considered (Merx, 1992).

2.3.2 Drag load

The explosion generates a pressure wind which acts as a drag load on smaller obstacles such as pipes and equipment (Bjerketvedt, et al., 1990). The drag acts on the back of the object visualized as a suction force in Figure 2-5.

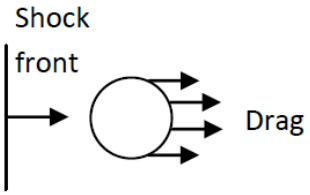

Figure 2-5 Drag load on the back of a small pipe.

The drag load or the drag pressure is represented by a drag coefficient which is dependent of the shape of the structure and which angle the load is "attacking" the object (Prud'homme, et al., 2013). The drag force can be estimated by Equation 2.3 where C_D is the drag coefficient, A [m^2] is the projected area of the object normal to the flow direction and $0.5\rho u^2$ is the dynamic pressure (Bjerketvedt, et al., 1990).

$$F_{drag} = C_D * A * 0.5 * \rho * u^2 \qquad (2.3)$$

The drag coefficient depends on the shape and orientation of the obstructing surface (ASCE, 2010). An overview of drag coefficients for different object shapes is found in Table 2-2.

Table 2-2 Drag coefficient for various object shapes (Baker, et al., 1983).

SHAPE	SKETCH	C_D
Right Circular Cylinder (long rod), side-on		1.20
Sphere		0.47
Rod, end-on		0.82
Disc, face-on		1.17
Cube, face-on	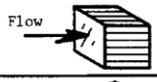	1.05
Cube, edge-on	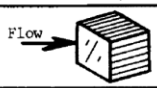	0.80
Long Rectangular Member, face-on		2.05
Long Rectangular Member, edge-on	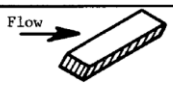	1.55
Narrow Strip, face-on	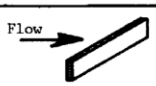	1.98

2.3.2.1 Shielding

The force on a slender object, e.g. pipe or RHS, downstream of another slender object is influenced by the wake generated by the upstream object (DNV, 2010). The drag force on the downstream object reduces due to this shielding effect. There are methods available to estimate the shielding effect, e.g. in Recommended practice DNV-RP-C205 Environmental Conditions and Environmental Loads published by DNV. The shielding factor η is a function of the spacing ratio α and the aerodynamic solidity ratio β. The shielding factor and definitions of the different parameters affecting it are presented in Table 2-3.

Table 2-3 Shielding factor (DNV, 2010).

Table 5-1 The shielding factor η as function of spacing ratio α and aerodynamic solidity ratio β.

β / α	0.1	0.2	0.3	0.4	0.5	0.6	0.7	0.8
< 1.0	1.0	0.96	0.90	0.80	0.68	0.54	0.44	0.37
2.0	1.0	0.97	0.91	0.82	0.71	0.58	0.49	0.43
3.0	1.0	0.97	0.92	0.84	0.74	0.63	0.54	0.48
4.0	1.0	0.98	0.93	0.86	0.77	0.67	0.59	0.54
5.0	1.0	0.98	0.94	0.88	0.80	0.71	0.64	0.60
> 6.0	1.0	0.99	0.95	0.90	0.83	0.75	0.69	0.66

The *spacing ratio* α is the distance, centre to centre, of the frames, beams or girders divided by the least overall dimension of the frame, beam or girder measured at right angles to the direction of the wind. For triangular or rectangular framed structures diagonal to the wind, the spacing ratio should be calculated from the mean distance between the frames in the direction of the wind.

The *aerodynamic solidity ratio* is defined by $\beta = \phi a$ where

ϕ = solidity ratio, see 5.3.2

a = constant

= 1.6 for flat-sided members

= 1.2 for circular sections in subcritical range and for flat-sided members in conjunction with such circular sections

= 0.6 for circular sections in the supercritical range and for flat-sided members in conjunction with such circular sections.

The effect of the arrangement and varying size of obstacles in a complex structure are not included in the shielding factor. Due to that, advanced CFD software such as FLACS is required to achieve a correct determination of the shielding effect (Bjerketvedt, et al., 1990). According to the limitations, CFD is not treated in this report hence the analyses performed are based on the recommended practice from DNV.

2.3.2.2 Turbulence

A deflagration can also be described as a type of explosion in which the shock wave arrives before the reaction is complete (because the reaction front moves more slowly than the speed of sound in the medium) (Daintith, 2008). In this report, only gas explosions are considered when referring to explosions. Before the explosion initiates there is a leakage of gas and an explosion takes place as this gas is ignited (Bjerketvedt, et al., 1990). When the gas cloud is ignited, a flame is created which starts as a laminar flame. This flame travels with a low velocity of about 3-4m/s into the unburned gas. In most accidental explosions the laminar flame will accelerate into a turbulent flame when the flow field ahead of the flame front becomes turbulent. This turbulence arises due to interaction between the flow field and obstacles such as equipment, piping, structures etc. Congested areas e.g. pipe racks, support flame acceleration and cause high explosion pressures (Hjertager, 1984).

There exists a relationship between flame speed and flow velocity which is studied at Christian Michelsens Institute in Bergen (Bjørkhaug, 1986). The results from the study conclude that there exists a correlation between these two phenomena as depicted in Figure 2-6.

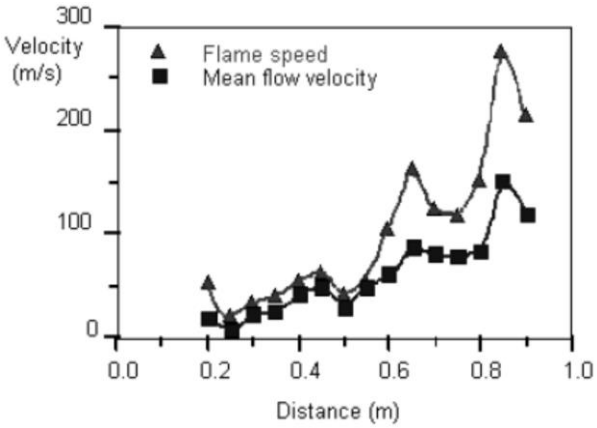

Figure 2-6 Relationship between flame speed and flow velocity (Bjørkhaug, 1986).

For comprehensible understanding of the concept presented above and the reason as to why drag pressure increases as a result of both turbulence and flow, the process is visualized as a positive feedback loop (Figure 2-7) as in GexCon's Gas Explosion Handbook (Bjerketvedt, et al., 1990). The first phase is the actual explosion which involves the combustion of gas leading to increased pressure in combination with an expansion of air. When this air wave travels over an obstacle, turbulence is generated which further enhances the combustion.

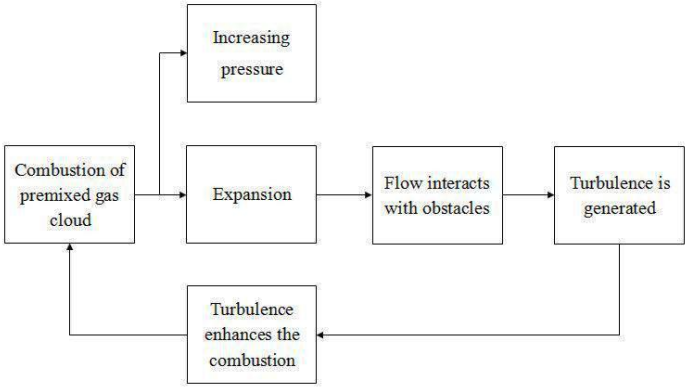

Figure 2-7 Positive feedback loop due to turbulence (Bjerketvedt, et al., 1990)

Reynolds number is a parameter that characterises if a flow is turbulent or laminar (Bjerketvedt, et al., 1990). It is referred to in Equation 2.4 where u is the flow velocity, L is the characteristic dimension of the geometry of the object and *v* is Poisson's ratio.

$$Re = \frac{uL}{v} \qquad (2.4)$$

An example of a cylinder in a cross flow is given in Figure 2-8. The flow is laminar if the Reynolds number and the flow velocity are low, and turbulent with vortices in the wake of the cylinder for higher Reynolds numbers.

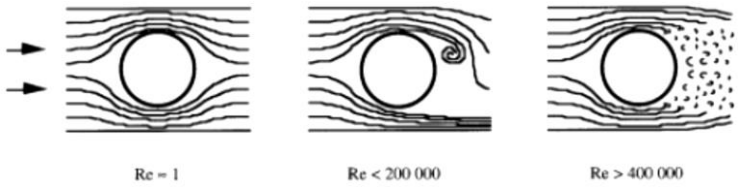

Figure 2-8 Cylinder in a cross flow at different Reynolds numbers (Bjerketvedt, et al., 1990).

2.3.2.3 Reliability of drag calculations

The matter of shielding and turbulence effects on the drag force is complicated. (Prud'homme, et al., 2013) raise attention to the fact that by studying available literature it is clear that there is a need for further study of how shielding and turbulence are affecting the drag coefficient. (Bjerketvedt, et al., 1990) also state that for non-stationary loads from gas explosions, the estimation of the drag load is uncertain and that it is probably dependent on several factors, e.g. turbulence level, time and pressure rise time. Furthermore, many investigators have reported that flow turbulence and cylinder surface roughness significantly affect the variation of C_D versus Re (Liu, et al., 2008). Moreover, when multiple cylinder shapes are involved the Reynolds number is more complicated to predict according to tests performed by (Liu, et al., 2008).

2.4 Utilized computer software

Throughout the work with this thesis a selection of computer software packages have been utilised in order to achieve the essential outputs. In Table 2-4, an overview of the software, the outputs relevant for the performed study and references to manufacturer are presented. In addition to the software presented in the table a selection of programs from the Microsoft Office package are utilized but not specified in this overview.

Table 2-4 Utilized computer software overview.

Name	Abbreviation	Relevant output	Reference
PDMS	Plant Design Management System	Pipe support loads, drawings, dimensions	www.aveva.com
Abaqus/CAE	Abaqus/Complete Abaqus Environment	Reaction forces, deflections, Eigen frequencies	www.simulia.com
STAAD.Pro	-	Utilization ratio of members, reaction forces	www.bentley.com

3 Design practise in NYX

There are internal AKSO documents for NYX describing and defining in detail all aspects of the design process relevant to the project. To provide the reader of this report with a brief understanding of the design process of pipe rack steel structures, a compiled description is presented in this chapter. It is worth mentioning that the design practise in NYX and the practise utilized in the performed studies differ. In NYX the DAF utilized in design is taken as one value of 1.5 for all structures, while in this study DAFs are calculated based on outputs from the FEA for each structure.

3.1 Load specification

In order to obtain the design loads, an advanced CFD analysis has been executed by Lloyd's Register Consulting in the explosion simulation tool FLACS. The results of the simulations form the basis of the internal AKSO document: Design of Accidental Loads Specification (DAL Spec). Among other important parameters related to blast load calculation, the DAL Spec. contains blast pressure distributions, magnitudes and durations for the structures at NYX. These parameters are used as input by the structural engineers in the design process and will also be utilized in the dynamic FEA performed in this study.

3.2 The design process

In this chapter, a brief summary of the design process for pipe rack steel structures in NYX is described. For the interested reader a more comprehensive description of the process is given in internal AKSO documents available on request.

The loads should be applied according to one of two available models.

- Uniform overpressure applied on specified surfaces:
  walls/floors/structures/large equipment.
- Drag peak pressure (ΔPd) on equipment/supports and free standing structures.

The choice of model depends on the size of exposed area in the direction of the blast. For open structures such as pipe racks this area is relatively small and the drag pressure model is therefore used for all studied structures. In addition it is considered that there will be no source of gas leak within the pipe racks; hence the blast load is assumed not to occur between various layers in pipe racks. Moreover, transverse loads are applied as linear loads to all main members of rows perpendicular to the blast direction and on bracings that are not parallel to the blast direction.

DAF and shape factor is multiplied by the blast load and the exposure area is taken as the projected area, which is obtained from the 3D models in the software PDMS as depicted in Figure 3-1. The weight of larger pipes are also collected from PDMS and applied in the positions of the pipe supports.

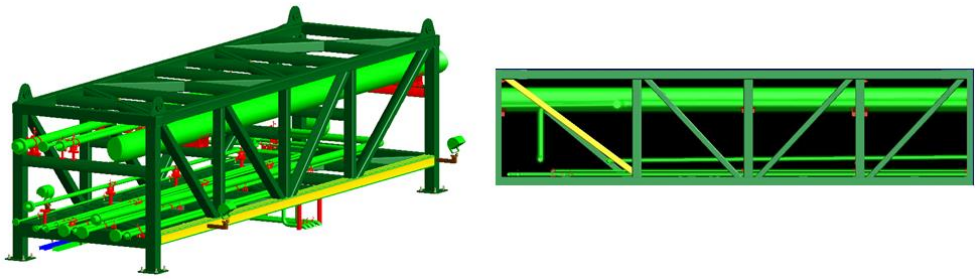

Figure 3-1 3D model of a pipe rack and its projected area obtained from PDMS.

Shielding effects are taken into account by applying 50 % of the blast load on secondary structures such as the back of a pipe rack, and turbulence is not considered. It is worth mentioning that this calculation procedure is not in accordance with the recommendations given in (DNV, 2010) and is not employed in this study.

3.3 Method of calculation

A static analysis using calculated design loads is performed to determine the dimensions of elements and global sizes required to withstand the applied loads. In NYX, and AKSO in general, this is done in the FE software STAAD.Pro. The calculations can be divided into six steps.

1. Determine Eigen periods (T) for the structure.
2. Obtain DAFs from Figure 1-3 assuming a blast load duration of 300ms.
3. Determine drag coefficient (C_d) according to EN 1991-1-4 Section 7.
4. Calculate design loads: $Q_d = \Delta P * C_D * A *$ DAF.
5. Apply design loads including the reduction due to shielding on secondary structures.
6. Run FEA using STAAD.Pro.

3.3.1 Simplified method

In order to speed up the calculation procedure a simplified method is recommended by AKSO to be applied for all structures in NYX. In the simplified method the assumption is made that all primary structures are in the elastic stress range i.e. no plasticity is allowed. Furthermore, the maximum DAF is used to calculate the relative dynamic blast loads for each element. The maximum DAF of 1.5 is taken as the highest value of the curve depicted in Figure 1-3, which is independent of the structures Eigen period. The representative dynamic loads are added as static loads to the FE models before running the analysis. Omitting the determination of the Eigen period saves a significant amount of time as a full dynamic analysis of the structure is subsequently not required. On the other hand, a consequence of adapting the simplified method is that the blast load is potentially over estimated and hence the resulting structures can be produced with overly conservative designs.

4 Structures to analyse

The chapter starts with a general definition of pipe racks and is followed by the selection of the pipe racks in NYX. After that the input to the analyses are presented together with the simplifications made to the models. Finally, the sought outputs from the analyses are presented.

4.1 Pipe racks

A pipe rack is an elevated truss structure used to support pipes, cables or other instrumental equipment as depicted in Figure 4-1. On NYX the majority of the trusses consist of rectangular hollow sections (RHS) of steel running horizontally between the supports, vertically between the frames and diagonally to stiffen and transfer loads horizontally and vertically. The use of RHS profiles is recommended practise by AKSO to achieve a construction friendly design. The trusses are supported by concrete columns transferring the reaction forces to the ground. The pipes are connected to the pipe rack with pipe supports shown in red in the figure below. The connections between steel and concrete are designed as pinned connections hence no moment is transferred between steel truss and concrete columns.

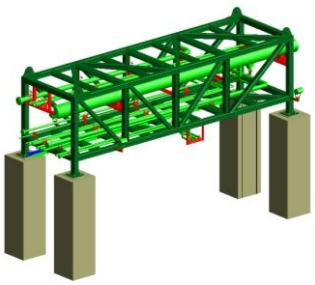

Figure 4-1 Steel pipe rack supported on concrete columns.

4.2 Choice of structures in NYX

Analyses are performed on three existing pipe rack steel structures from NYX selected because of their significant differences in span length, height, width and pipe arrangement (Table 4-1).

Table 4-1 Dimensions and total weight of the NYX structures

Structure	R56AV01	R56BV01	R44GV01
Length (m)	43.95	15.27	33.60
Height (m)	5.00	3.45	2.00
Width (m)	6.00	4.20	2.00
Total weight (kg/m)	4871	2340	2670

The length of the structures varies between about 15 meters to 44 meters with different heights and widths. The three pipe racks are illustrated in Figure 4-2 without pipes and equipment. They all have RHS profiles which are of majority on NYX. Limiting the choice of profiles is also convenient when evaluating the results of the analyses as the number of parameters is reduced. When choosing the structures only one-level pipe racks are studied to further limit the variation of parameters. Structure R56AV01 has pipes distributed on both the top and bottom frames while R56BV01 only has pipes on top and R44GV01 only on the bottom frame.

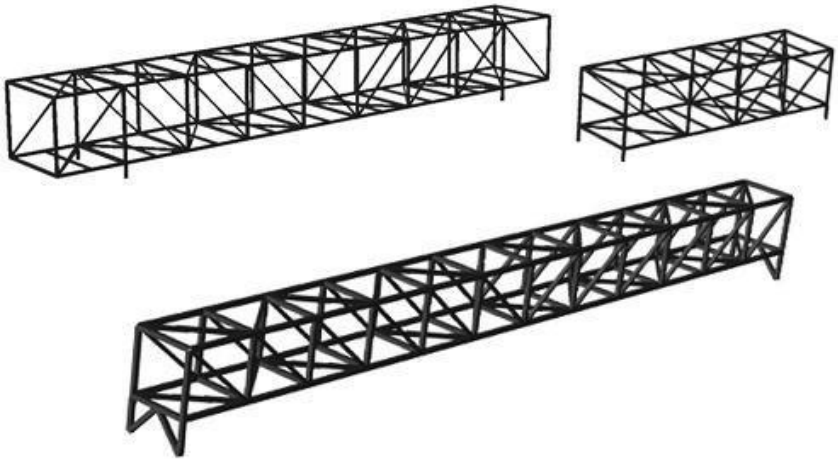

Figure 4-2 Pipe racks R56AV01, R56BV01 and P44GV01 (left to right).

4.3 Input to analysis

The self-weight of both structural elements and pipes are given the gravity constant $g = 9.81\,\frac{m}{s^2}$, and a density $\rho = 7850\,\frac{kg}{m^2}$. The pipe self-weight is calculated based on the pipe point loads from the 3D models in PDMS and applied to the FE models as inertia masses in Abaqus/CAE. An example of the pipe load calculations for the NYX structure L56BV01 is presented in Appendix B – Point blast loads.

In Appendix A – Blast load calculations, a calculation example of the blast loads for L56BV01 is presented. The blast loads are calculated based on DNV RP C205 (DNV, 2010) and DAL Spec. The loads are separated between the blast loading of the structural elements (RHS) and the pipes. The blast loads on the RHSs are applied as distributed loads acting transversally on the structure.

4.4 Simplifications in modelling

Throughout the work with the thesis the authors strive to reduce conservatism in the results. However, when modelling the structures in Abaqus/CAE, some simplifications are required in order to make the modelling less complicated. These simplifications with explanations are presented in the following section.

Equipment

All equipment other than pipes is neglected. The effect of the blast load acting on the equipment can be neglected as the exposed area and the mass of the equipment is small in comparison with the actual structure.

Load application

The pipes are not designed to contribute to the overall stiffness of the structure and are therefore modelled as inertia masses in the same position as the pipe supports. In the pipe support positions transverse point loads are placed to represent the blast load on the pipes. The blast loads are taken as the distributed blast load over the pipes times half the distance between adjacent pipe supports as illustrated in Figure 4-3. The shielding effects from the front frame and from the pipes are included when calculating the blast point loads.

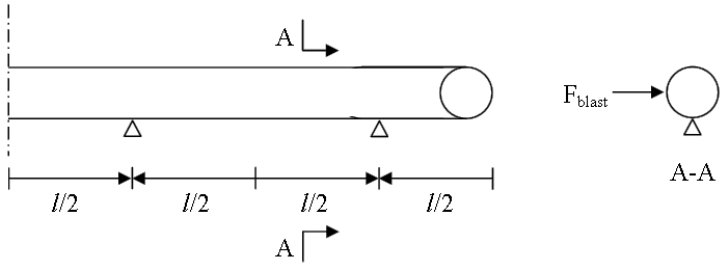

Figure 4-3 Pipe section and profile. Half of the distributed blast load from each span is concentrated as one point load in the position of each pipe support.

The structures are analysed with blast load durations spanning from 50 ms to 500 ms, hence the time required for the blast to travel between the front and back frame is short. It is therefore assumed that the time required for the blast load to travel between the adjacent frames $\Delta t = 0$, i.e. the blast load acts on the front and back frame simultaneously. A study to evaluate the effects of the assumption is found in Appendix C and indicates that assuming $\Delta t = 0$ is conservative.

Pipe supports

The pipes are modelled to have their centre of gravity on the top or bottom RHSs. All pipes of prominent size are attached to the structure by pipe supports as illustrated in Figure 4-4. The distance between the centre of the pipe and centre of the structure generates a moment in the RHS members illustrated in Figure 4-4. However, as the result of interest in the analyses is the global behaviour of the structure, the relatively small eccentricities (e<500 mm) causing a local moment in the transvers RHS members are neglected when modelling the structure.

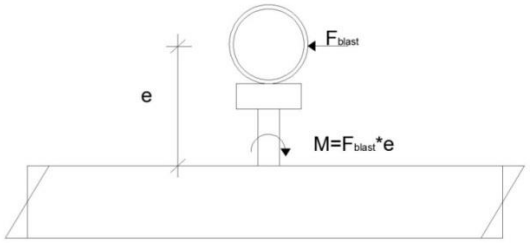

Figure 4-4 Induced moments in the RHS caused by blast load on pipe.

Blast

Both drag peak pressure (ΔPd) and duration are taken directly from DAL Spec. before applied to the analyses. From DAL Spec. the peak pressure for the studied structures is set to 0.1 for a blast duration of 300 ms. When analysing the structures the duration is varied from 50 to 500 ms and the peak pressure are set to 0.1 bar i.e. without taking the probability of these magnitudes into account. It is conservative to assume that all durations are equally probable and that a peak pressure of 0.1 bar occurs for all durations. Regarding blast duration and peak pressure no limitations are found relating to these factors and their likelihood beyond what is included in the DAL Spec.

Shielding and turbulence

Blast loads, including turbulence and shielding effects, are calculated according to the guidelines given in DNV recommended practise (DNV, 2010). When adapting the formulas and tables from the recommended practise the following simplifications are made.

- The angle between the wind direction and the axis of the exposed member is set to 0. This gives no reduction of the wind force resulting in a conservative assumption.
- When calculating the aerodynamic solidity ratio (β) a separation between circular sections and flat-sided sections is recommended. For the part of the structures where both circular pipes and flat-sided members are present, β is chosen with regard to what sections are in the majority in that specific case.
- Increased turbulence caused by the diagonals in the same plane as the combination of flat-sided members and circular members is disregarded. These members are not perpendicular to the wind direction and have a small contribution to the turbulence effect compared to the perpendicular members (flat-sided and circular) in the same plane.

Small pipes

A majority of all pipe loads where the pipe has a diameter less than 100 mm are neglected in the analyses. The pipe loads are taken directly from the 3D model in PDMS and because some of the structures are not completed, most of the pipe loads from the small pipes are still not given. Calculating the weight of the pipes is complex and time consuming because content, pressure, angles etc. need to be evaluated. In addition, loads for some of the pipes with a diameter less than 100 mm are specified in PDMS but as these values are small in comparison with the normal sized pipes, it is reasonable to neglect them.

Modelling of concrete supports

The chosen pipe racks are supported on concrete columns but since the behaviour of the steel structure is of interest, the columns will not be analysed. This separation is also in accordance to the project organisation in NYX as concrete structures are designed by the Civil Department and structures in steel are designed by the Structural Department. The connection between the concrete supports and the steel pipe rack is designed with base plates and bolts and are modelled as pinned connections in the analyses.

4.5 Sought outputs from analysis

To calculate DAFs for the structures, base shear (BS) and overturning moments (OT) are used and therefore the following outputs are required:

- Eigen frequency (f)
- Eigen period ($T = \frac{1}{f}$)
- support reactions in transversal direction, i.e. BS
- support reactions in longitudinal direction to calculate OT.

A description of how the BS and OT are defined is found in Figure 4-5.

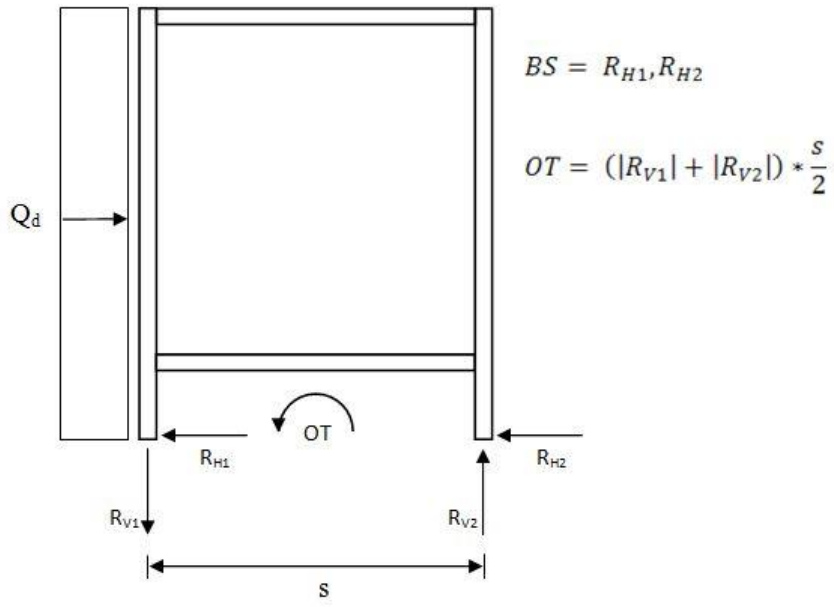

Figure 4-5 Pipe rack cross-section exposed to explosion load Q_d with support reactions R_H and R_V.

5 FEA in Abaqus/CAE

In order to perform transient dynamic analyses of the structures in NYX the FEA software Abaqus/CAE is utilized. CAE is an abbreviation of Complete Abaqus Environment and consists of the Abaqus software application package with modelling, processing, analysing and visualisation tools in the same program. Abaqus/CAE is the most established software for FEA in AKSO as well as one of the most used software for engineers worldwide. The content of the chapter is based on the Abaqus/CEA User's Manual available online.

According to DNVs recommended practise, a FEA should require a descriptive documentation in order to allow for independent verification by a third party (DNV, 2013). The recommended documentation form the setup of this chapter so that the result will be in accordance with the recommended business standard and include general geometry, boundary conditions (BCs), element type and mesh, material properties and loads as well as supplementary assumptions such as blast duration and damping. In Figure 5-1 the FE model of the pipe rack structure R56BV01 with applied loads and BCs is illustrated.

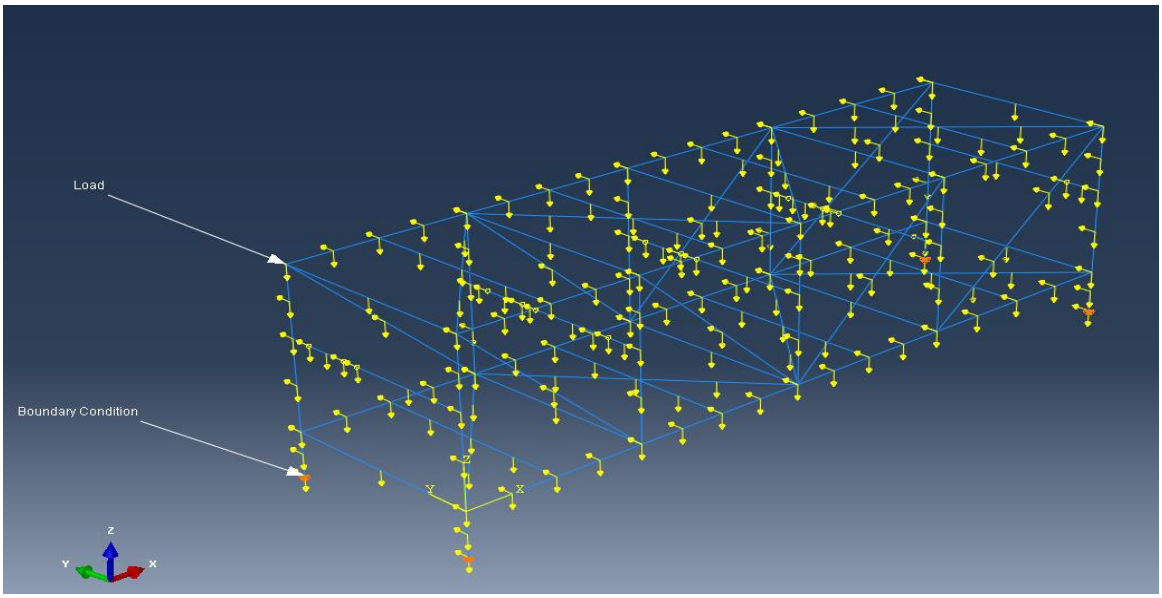

Figure 5-1 FE model of structure R56BV01 in Abaqus/CAE. Yellow arrows represent loads and orange dots BCs.

5.1 Geometry model and boundary conditions

The chosen structures are modelled in Abaqus/CAE based on drawings available in AKSOs internal documents. The drawings include overall dimensions and element properties needed to model the structures. A model in Abaqus/CAE consists of a number of parts connected by BCs where all parts are given attributes in accordance with Figure 5-2. Parameters are chosen to achieve a simplified representation of the real structure while keeping the sought outputs in mind. For example, the "Planar Wire Shape" is chosen in the part definition in Figure 5-2. This simplification represents the global dynamic behaviour well even though the representation of details such as joints

and welds become simplified. All BCs representing the connections between the steel pipe racks and concrete columns as depicted in Figure 4-1 are designed as pinned; hence pinned connections are adapted in the FE model for these types of connections.

5.2 Choice of elements and meshing

Truss elements are preferred when representing axial stiffness while beam elements are in addition representing bending stiffness. The structures are therefore modelled as beam elements in analyses. Moreover, all pipes are modelled as inertia masses since they are not contributing to the overall stiffness of the structure (ref. Chapter 4 Section 4.1). Inertia loads are non-structural masses contributing with inertia to the dynamic behaviour of the overall structure and are added in the Part-module (Figure 5-2).

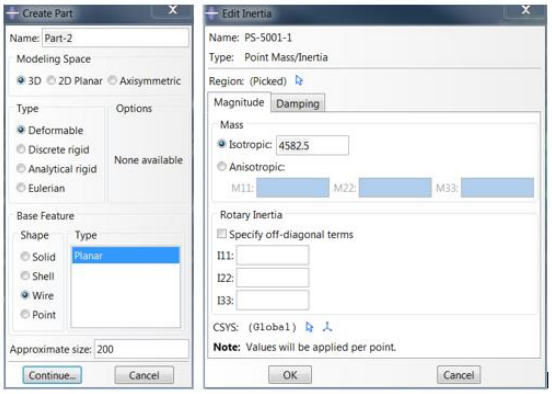

Figure 5-2 Part definition and inertia editor.

The mesh of the FE model is generated using the mesh module. Various levels of automation and control are available in Abaqus/CAE to give the user the possibility to generate meshes representing the real behaviour of the structure. It also allows the user to control the CPU[4]-time needed to perform the analyses. In order to determine a suitable mesh for the structure, a convergence study is executed for structure R56BV01. The convergence study settles the number of elements needed as well as the approximate global mesh size (AGMS). By studying Figure 5-3 it is concluded that a convergence is achieved with a mesh of approximate 1300 elements and an AGMS of 0.2.

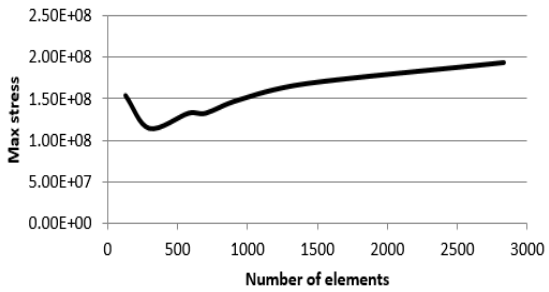

Figure 5-3 Convergence study of mesh for structure R56BV01.

[4] Central Processing Unit

5.3 Material models and properties

All structures are designed with steel S355 and a non-linear behaviour as illustrated in Figure 5-4. There are different ways of measuring the stress and strain for steel. From material testing the results are often given as "engineering" stress-strain curves, while for use in FEA the "true" stress-strain curves are recommended (DNV, 2013). For that reason the "true stress" is used for all analyses presented in this report. Figure 5-4 is generated from values given in (DNV, 2013) and illustrates the difference between "true" and "engineering" stress-strain relationships for S355.

5.4 Loads and load sequences

The load and load sequences in Abaqus/CAE are organised as steps in order to define specific parameters such as loads and BCs for separate sequences of the analyses. In the performed analyses the load sequences are divided into three steps; initial, self-weight and blast load and given values as presented in the following sections.

5.4.1 Initial step

In the initial step the BCs for the structure are created. These BCs are in the succeeding steps propagated from the initial step as they maintain constant throughout the analyses. The setup in the "Boundary Condition Manager" is depicted in Figure 5-5.

5.4.2 Self-weight step

The self-weight step is defined as "Static, General" and the load amplitude set to "ramp" to model the self-weigh as a static load. The ramp-function is a built-in function in Abaqus increasing the load magnitude linearly over the step. By using the ramp-function, the load is applied without creating a mass acceleration of the structure which can cause an oscillation of the structure. Oscillation will disturb the dynamic behaviour of the structure and cause errors in the results. To demonstrate this, the von Mises stresses for a selected element in structure R56BV01 with both "ramp" amplitude and instant loading are illustrated in Figure 5-4. The self-weight is applied during the first second (0-1 s).

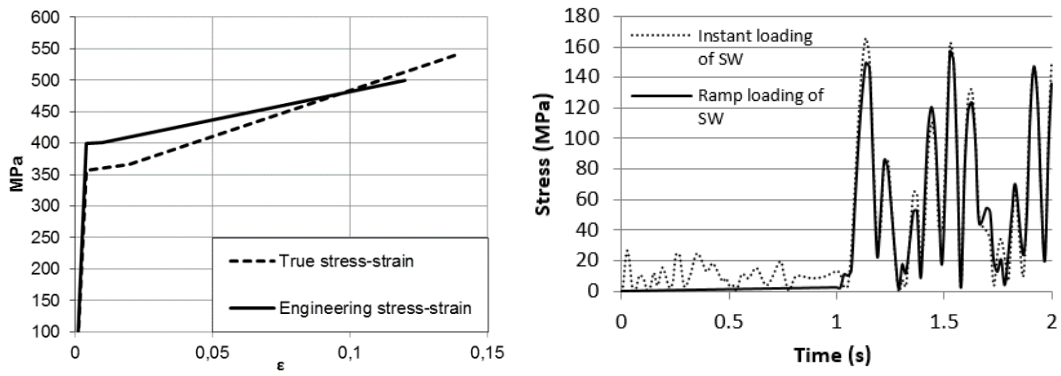

Figure 5-4 Proposed stress-strain curve for S355 (DNV, 2013) and Von Mises stresses for a random element of structure R56BV01 - blast duration 200ms.

5.4.3 Blast load step

The blast load step is defined as “Dynamic Implicit” and the loads are applied with a triangular blast pulse curve. Dynamic analyses in Abaqus/CAE can be done either by choosing “Dynamic implicit” or “Dynamic explicit” as calculation procedure. Without going into details in the differences between the two methods, the implicit calculation procedure uses a simpler algorithm for the analyses than the explicit, resulting in a reduced CPU-time. As the pipe racks on NYX are fairly simple and modelled with beam elements, an implicit calculation procedure can safely be chosen. Moreover, choosing the implicit integration instead of the explicit allows the user to change the step from dynamic to static without remodelling the structure in the program. To learn more about dynamic calculation procedures in Abaqus/CAE, the reader is recommended to familiarize further with the Abaqus/CEA User’s Manual.

To obtain a smooth DAF-curve, the FE-analyses are executed with blast durations varying from 50 ms to 500 ms. By retaining the structural stiffness, the structural Eigen period is kept constant and the only variable in the analyses is the blast duration. The blast duration is changed by defining the amplitude of the blast pulse in the amplitude toolbox in Abaqus/CAE as depicted in Figure 5-5. In accordance with Biggs curve, the blast pulse is defined as a triangular symmetric pulse.

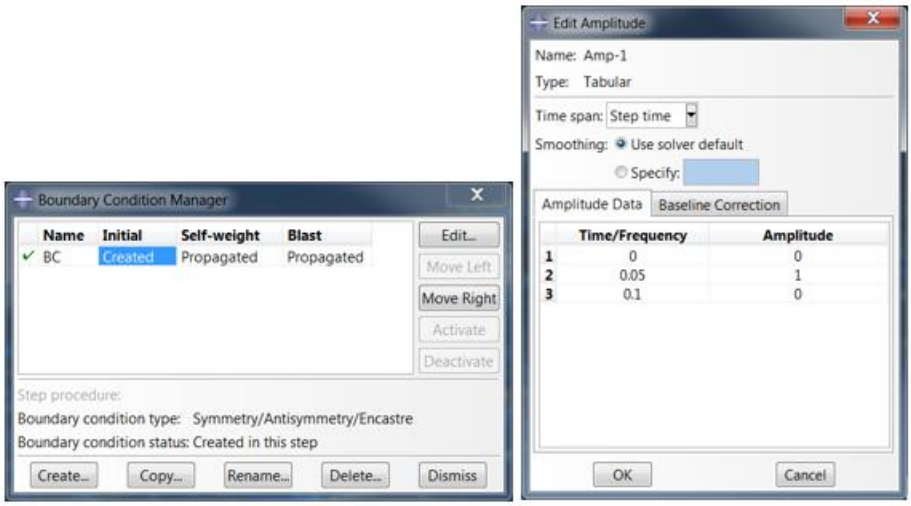

Figure 5-5 BC manager and amplitude toolbox.

6 Results

The results from the FEA of the NYX structures are presented in this chapter. The first section presents the results from analyses, while the results are verified in the second section in accordance with recommendations given in (DNV, 2013).

6.1 Output from FEA

A summary of the input for the structures and their output values from the FEA is presented in Table 6-1. In the sixth row from the top the aspect ratios (AR) of the structures are presented.

Table 6-1 Output values from finite element analyses of the NYX structures.

Structure	R56AV01	R56BV01	R44GV01
Geometry			
Length (m)	43.95	15.27	33.60
Height (m)	5.00	3.45	2.00
Width (m)	6.00	4.20	2.00
Aspect ratio	1.20	1.22	1.00
Tot. weight per unit length (kg/m)	4871	2340	2670
Distributed pipe mass on top (%)	60	100	0
Distributed pipe mass on bottom (%)	40	0	100
Output values			
Eigen frequency (Hz)	4.154	4.426	4.722
Eigen period, T (s)	0.241	0.226	0.212
Maximum DAF-values			
Base shear, BS	1.27	1.37	1.32
Difference from (Biggs, 1964) curve	0.85	0.91	0.88
Overturning moment, OT	1.72	1.39	1.26
Difference from (Biggs, 1964) curve	1.15	0.93	0.84

AR represents the ratio between the height (*b*) and width (*s*) of the structure according to Figure 6-1. DAF-curves based on BS and OT for each structure is presented in Figure 6-2.

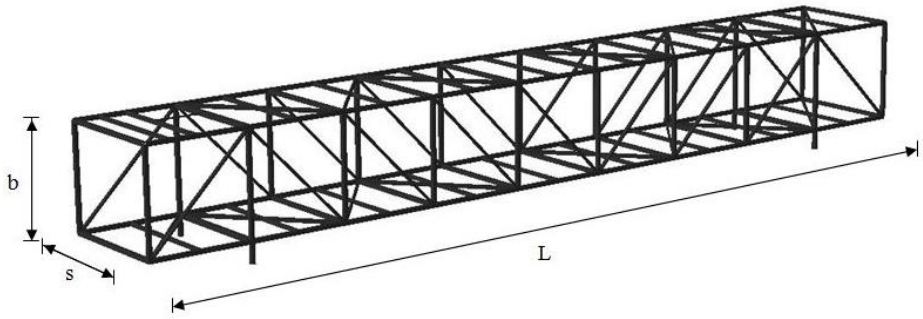

Figure 6-1 Notations of geometric entities.

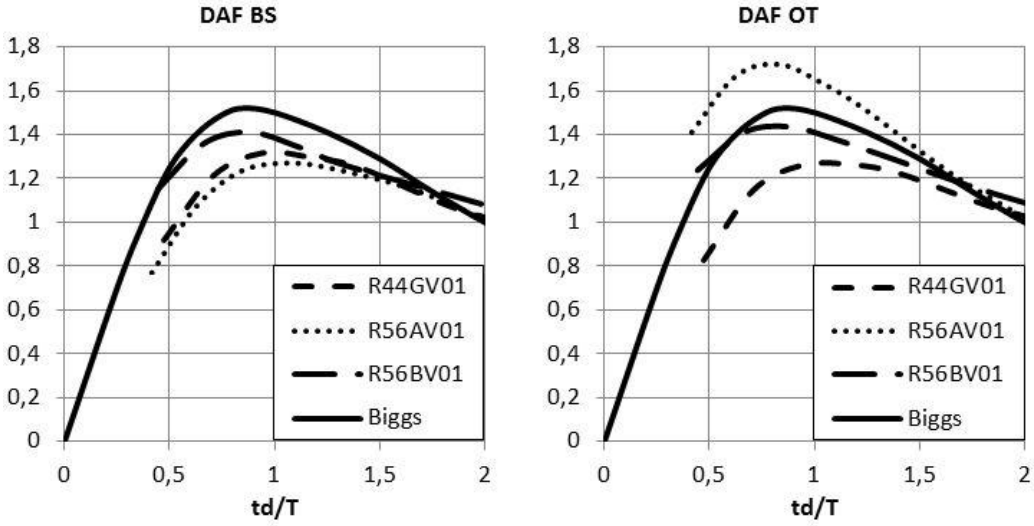

Figure 6-2 DAF-curves for the NYX structures.

6.1.1 Maximum DAFs

When studying Figure 6-2 and the DAF-curves based on BS, all curves lay 9-15 % below the Biggs-curve's maximum. The lowest DAF-curve is found for structure R56AV01 and the highest for R56BV01. For curves based on OT, the R56AV01 structure has the highest curve with a maximum 15 % higher than the Biggs-curve. Both structure R56BV01 and R44GV01 lay below the Biggs-curve with maximum DAFs 7 % and 16 % less than the Biggs.

6.1.2 Parameters

Results sorted by length and pipe mass distribution versus DAF-curves based on BS and OT, are found in Table 6-2.

Table 6-2 Results sorted by length and pipe mass distribution vs. DAF-curves.

		DAF_{BS}-curve			DAF_{OT}-curve		
Parameter		High	Mid	Low	High	Mid	Low
Length	Long			x	x		
	Mid		x				x
	Short	x				x	
Pipe mass distribution (top/bottom)	60/40			x	x		
	100/0	x				x	
	0/100		x				x

6.2 Verification of FEA

To verify the Abaqus model, a static check of whether the horizontal reaction forces are of the same magnitude as the applied loads is performed. The result of the verification is presented in Table 6-3 and the ratios are close to 100 %.

Table 6-3 Verification of FEA comparing reaction forces to applied loads.

Structure	Horizontal reaction forces from Abaqus [kN]	Applied loads [kN]	Ratio [%]
R56AV01	2246.4	2120.3	94.4
R56BV01	363.9	350.6	95.5
R44GV01	817.3	762.8	93.3

7 Discussion of results

When studying the results from the analyses of the NYX structures the analyses indicate that the dynamic response is not simply quantified by one single value but is different for the two sets of support reactions, i.e. the base shear and the overturning moment. This chapter starts by evaluating these results and concludes that a parametric study is required to gain better understanding of the correspondence between the structural behaviour and the studied parameters. Later in the chapter, the results from the parametric study are presented and discussed. To include new results in a discussion is non-conventional. The parametric study and its results are however presented in this chapter as they are a consequence of the discussion of the analyses and results of the NYX structures.

7.1 NYX structures

From the result of the analyses it is concluded that the Eigen periods are close in range (0.212 - 0.241 s), the ARs are similar (1.00 - 1.22) and they are built-up by similar cross-sections. A conclusion that can be drawn from this is that none of these parameters seem to influence the shape of the DAF-curves.

7.1.1 DAFs based on BS

Structure R56BV01 has the highest maximum DAF-value based on BS followed by R44GV01 and R56AV01. It looks as though the distribution of the pipe mass is not representative for the DAF-curves. This leaves us with two parameters that could influence the DAFs; total weight per unit length (TWUL) and structural length.

Structure R56AV01 has about twice the TWUL than the other two structures and does also have the highest DAF-curve. R56BV01 and R44GV01 have almost the same TWUL but their DAFs are close in range. Hence, the TWUL does not seem to be related to the difference between the curves. The shortest structure has the highest DAFs and the curves decrease with increasing length. An assumption that shorter structures have higher DAFs is therefore reasonable.

7.1.2 DAFs based on OT

For the DAF-curves based on OT, R56AV01 reveals the highest DAFs and R44GV01 the lowest. The length of the structures does not seem to be representative for the distribution between the curves since the longest structure has the highest curve and the shortest structure has the second highest curve. The same holds true for the TWUL; the structure with the highest TWUL has the highest curve, but there is a difference between the two structures with similar TWUL.

R56AV01 is the only structure with distributed pipe mass while the pipe mass is concentrated to the top or bottom frame on the other structures. This could explain the variation between the curves concluding that structures with concentrated masses lay below the Biggs-curve.

7.1.3 Difference between BS and OT

There is a clear difference between the presented DAF-curves based on BS and OT. As the distribution of the curves does not follow the same pattern when based on BS and OT, it is difficult to make any predictions of what parameters that are influencing the DAFs in general. For that reason a thorough parametric study is required to investigate the influence of the parameters in detail.

7.2 Parametric study

The parameters which will be presented in Section 7.2.1 are chosen keeping the objective of the thesis in mind and endeavour results that will be applicable for future projects. In order to concentrate on how DAF changes with the different parameters, only structures with three types of RHSs are studied. What cross-sections assigned to the different parts of the structures are illustrated in Figure 7-1 and are limited to:

1) RHS300x200x12.5 in all diagonals
2) RHS300x300x30 (built-up profile) in vertical members over supports
3) RHS300x300x12.5 in horizontal and vertical members except those of point 2).

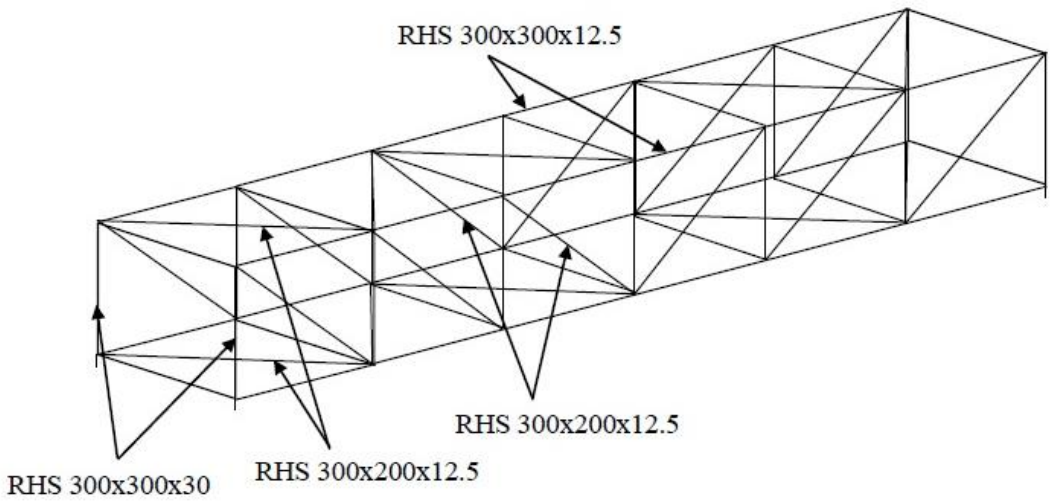

Figure 7-1 Fixed assignment of cross-sections for all structures.

To simplify the modelling in Abaqus all structures are modelled with one pipe on the top frame and one on the bottom as illustrated in Figure 7-2. It is worth mentioning that the weight of the pipes is one of the varied parameters, even though the diameter and number remain constant. More information regarding the varied parameters will be presented in the next section.

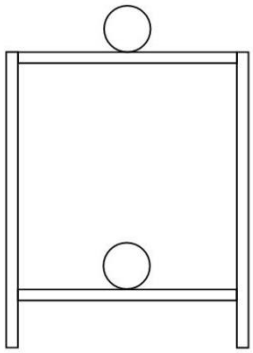

Figure 7-2 Pipe placement for models in parameter study.

In addition to these restrictions, the same simplifications as for the NYX structures presented in Chapter 4 Section 4.4 are valid for the structures modelled in the parametric study.

7.2.1 Choice of parameters and matrix

The possibility of combining parameters is numerous and a discussion evaluating the different parameters is required. The values of the parameters are defined after reviewing a great selection of pipe racks in NYX. This review in combination with evaluation of which values that would most likely be used for structures in future projects, determined the choice of parameters. Considering these aspects the chosen parameters are presented in Table 7-1.

Table 7-1 Geometric parameters in parametric study.

Aspect ratio, AR (b/s)	Structural length, L [m]	Pipe mass distribution (top/bottom) [%]	Pipe mass [% of total mass]
5/3	10	70/30	57 (high)
5/5	30	50/50	37 (low)
3/5	50	30/70	

These four parameters can be combined in 54 ways creating a matrix of models/structures as presented in Table 7-2. In order to verify the results and reduce the risk of errors in the calculations, a cross check is performed. This is utilized by analysing several of the models individually and comparing them between the two authors.

Table 7-2 Parametric matrix of models (1-54).

Geometry		Mass of pipes High = 57% of total mass Low = 37% of total mass	Mass distribution (top/bottom)		
AR	*L* [m]		70/30	50/50	30/70
5/3	10	High	1	2	3
		Low	4	5	6
5/3	30	High	7	8	9
		Low	10	11	12
5/3	50	High	13	14	15
		Low	16	17	18
5/5	10	High	19	20	21
		Low	22	23	24
5/5	30	High	25	26	27
		Low	28	29	30
5/5	50	High	31	32	33
		Low	34	35	36
3/5	10	High	37	38	39
		Low	40	41	42
3/5	30	High	43	44	45
		Low	46	47	48
3/5	50	High	49	50	51
		Low	52	53	54

7.2.2 Results

After completing the 54 FE-analyses and studying the results, certain tendencies regarding both DAF-curves and maximum DAF are obvious. The comparisons presented in the following sections illustrate the most interesting findings. Firstly, the differences between DAF-curves calculated based on OT and BS will be evaluated. Secondly the variations related to mass distribution, AR and total mass, length as well as Eigen period will be presented for both cases (based on OT and BS). The results presented in this chapter will form the basis for the discussion of the results presented in Section 0 as well as the conclusions drawn in Chapter 8.

7.2.2.1 Determination of DAF

In Figure 7-3, DAFs for models 16 to 30 (ref. Table 7-2) are presented based on BS and OT respectively. The choice of models is made in order to represent a general tendency in the study. From these figures a dissimilarity regarding both the DAF-curves and the maximum DAFs is obvious. The variation in the maximum DAFs calculated for BS are clearly lower than the ones calculated based on OT, where a majority of the DAF-curves is even exceeding the DAF-curve for a SDOF-system (ref. Figure 1-3).

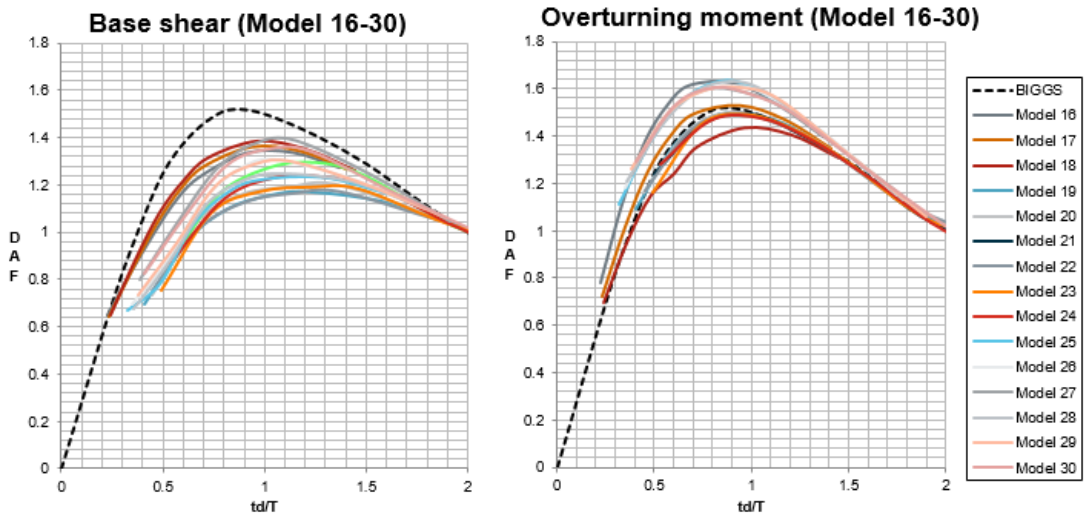

Figure 7-3 DAF-curves for models 16 to 30 based on BS and OT.

To illustrate this, variation four models are investigated; two with large variation between DAF-curves and two with small variation. Figure 7-4 presents DAF-curves based on both OT and BS for these models. From the figure it is clear that model 13 and 28 have a markedly larger difference between the DAF-curves compared with model 15 and 18.

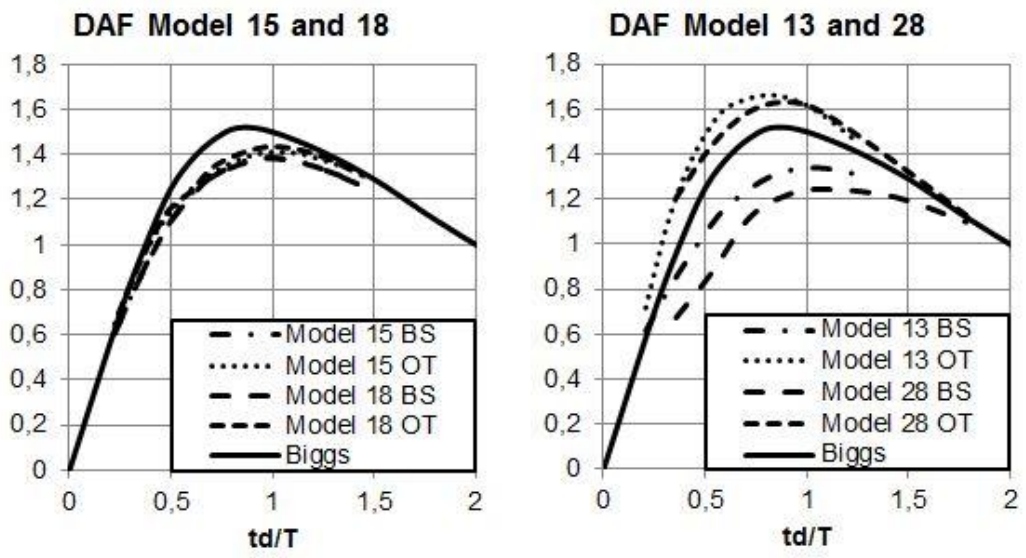

Figure 7-4 A selection of models with DAF calculated based on BS and OT.

By studying the parameters of the models further it is found that both model 13 and model 28 has a concentration of mass in the top of the structure (pipe mass distribution 70/30) while model 15 and 18 has the opposite (30/70). This correlation between pipe mass distribution and DAF-curves based on BS and OT require further investigation in order to find a pattern.

7.2.2.2 Mass distribution

Before the correlation between DAF-curves (BS and OT) and mass distribution is presented, the effect of mass distribution is presented separately for BS and OT. Aiming to evaluate whether the load distribution on the pipe rack affects the structural behaviour of the structure, DAF-curves with varying load distributions and ARs are presented in Figure 7-5 and Figure 7-6. The length of the structures is varying horizontally in the figures. By retaining the length, mass and AR within the individual figures and only varying the pipe mass distribution, a tendency is obvious. It is clear that load distribution 70/30 is resulting in the lowest DAF-curves as well as the lowest maximum DAFs for all variations of length and AR for BS. However, the opposite holds for OT as 30/70 results in the lowest values.

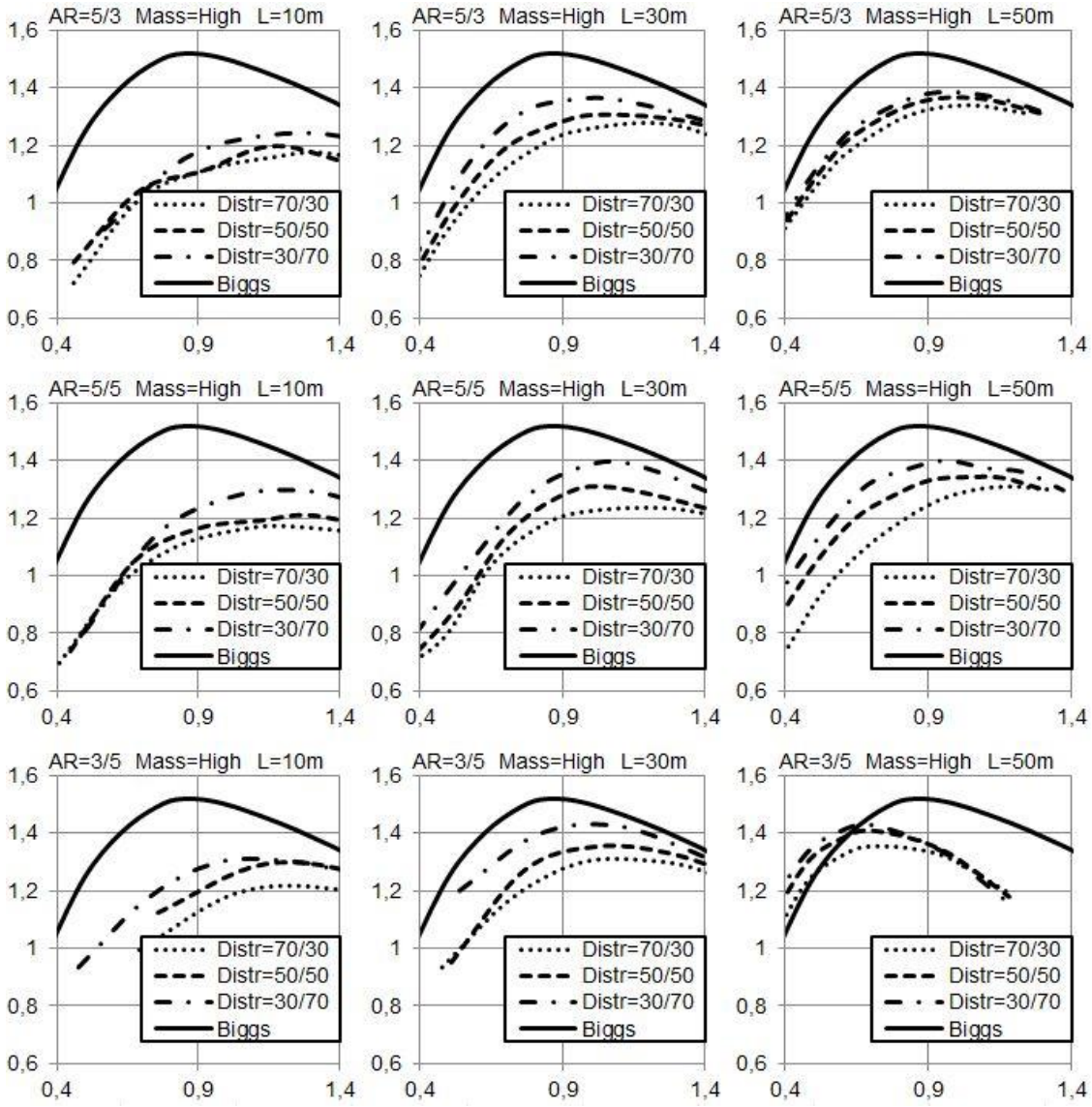

Figure 7-5 Variation of DAF based on BS related to mass distribution (DAF vertical axis – td/T horizontal axis).

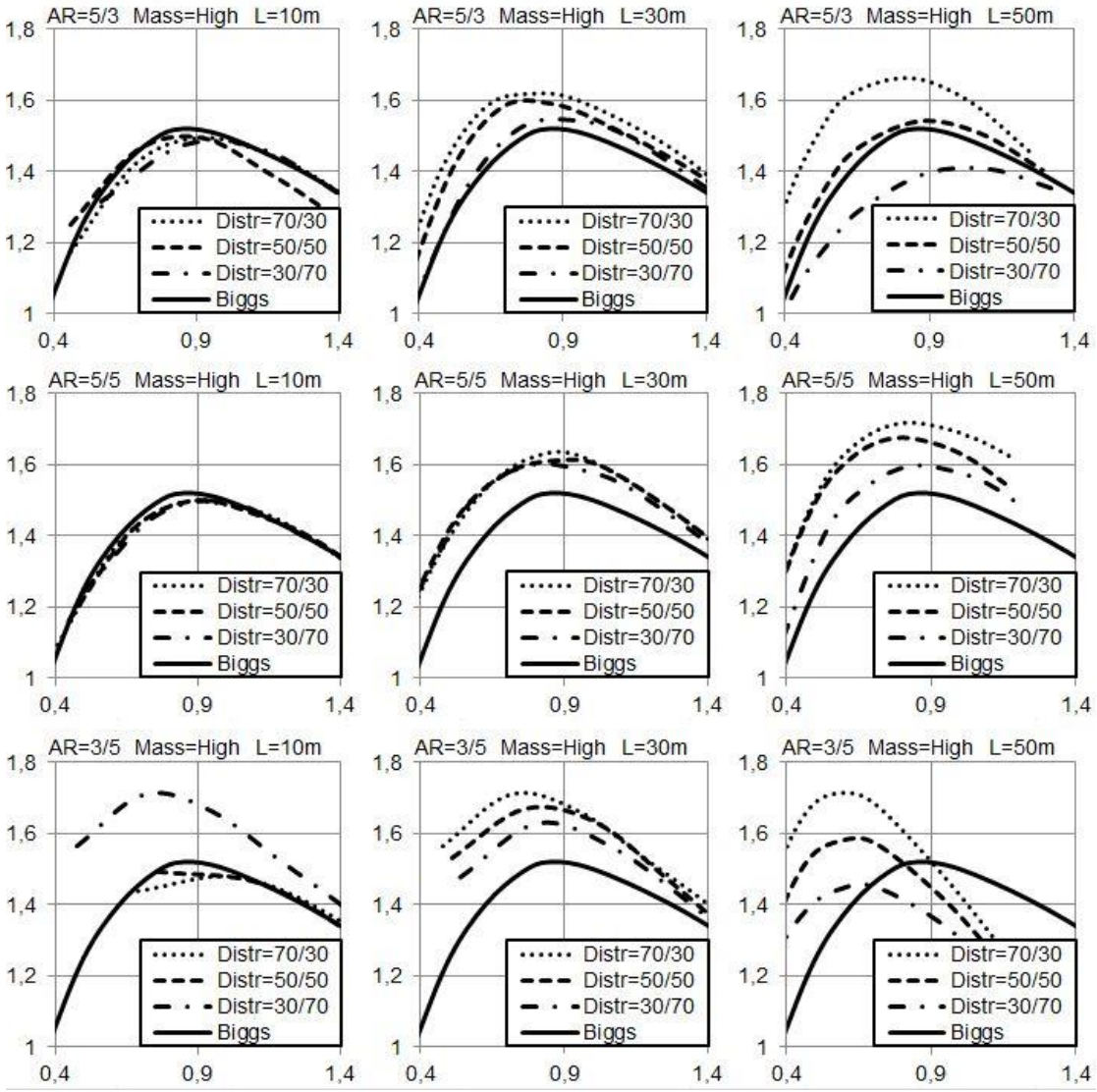

Figure 7-6 Variation of DAF based on OT related to mass distribution (DAF vertical axis – td/T horizontal axis).

As a supplement to the curves presented in Figure 7-5 and Figure 7-6, sensitivity analyses for the maximum DAF related to load distribution are performed. The sensitivity analyses are presented in Figure 7-7 and show a clear trend; from the DAF-curves based on BS the highest DAFs are achieved for the 30/70-distribution while the lowest for 70/30. Hence, by excluding a mass distribution of 30/70, the maximum DAF based on BS can be limited to 1.37. For OT on the other hand, the pattern is a bit different. For structures with medium to long Eigen period (correlates to some extend to structural length) the trend is that a 70/30 distribution reveals higher DAFs, i.e. the total opposite of DAF based on BS. Furthermore, for 30/70-distribution the maximum DAF irrespective of BS or OT is 1.63, with significantly lower maximum values found in both the low and the high end of the investigated Eigen periods T

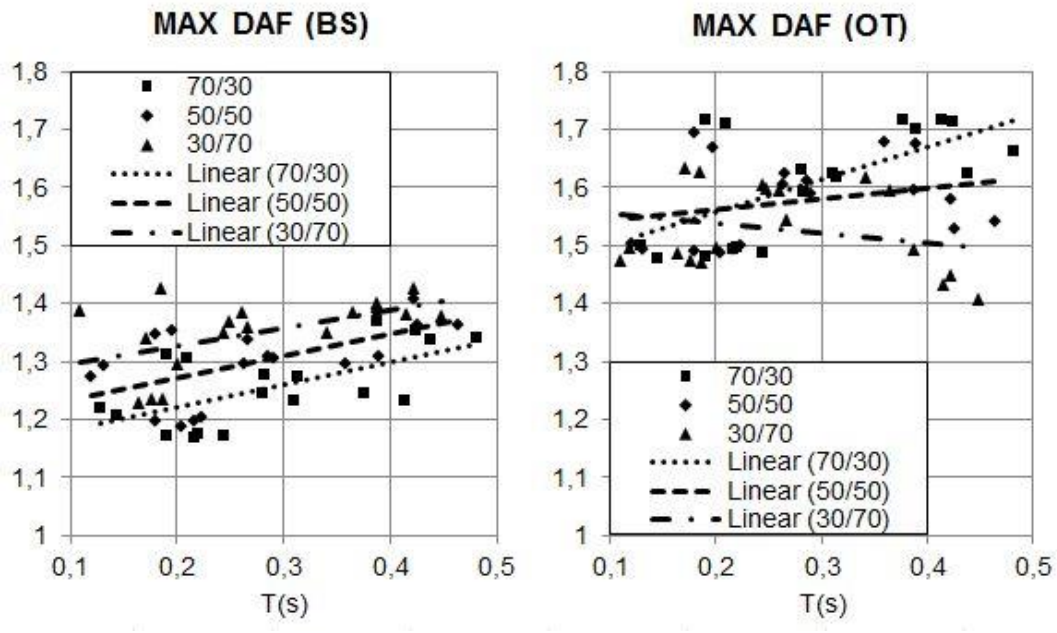

Figure 7-7 Sensitivity analyses of maximum DAF related to load distribution.

When a polynomial trendline is created for the 30/70 distribution for the DAFs based on OT, interesting results are revealed. From Figure 7-8 it is obvious that if choosing a 30/70 distribution, it is wise to also design a structure with either low or high Eigen period as that result in a lower maximum DAF.

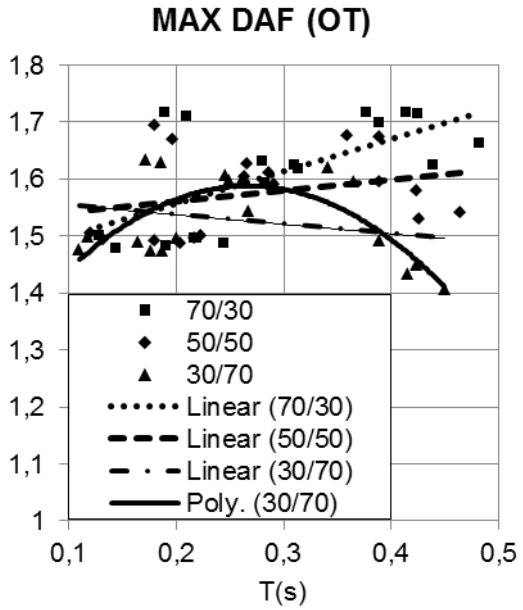

Figure 7-8 Polynomial trendline for the 30/70 distribution for maximum DAFs based on OT.

From these results it becomes clear that the mass distribution is affecting the dynamic behaviour when studying both BS and OT. However; how, why and to what extent this affects the DAF is still not clear. For this reason, the ratio between the CoM coordinate

and the resulting force[5] (RF) coordinate is plotted against the ratio of DAF calculated based on BS and OT.

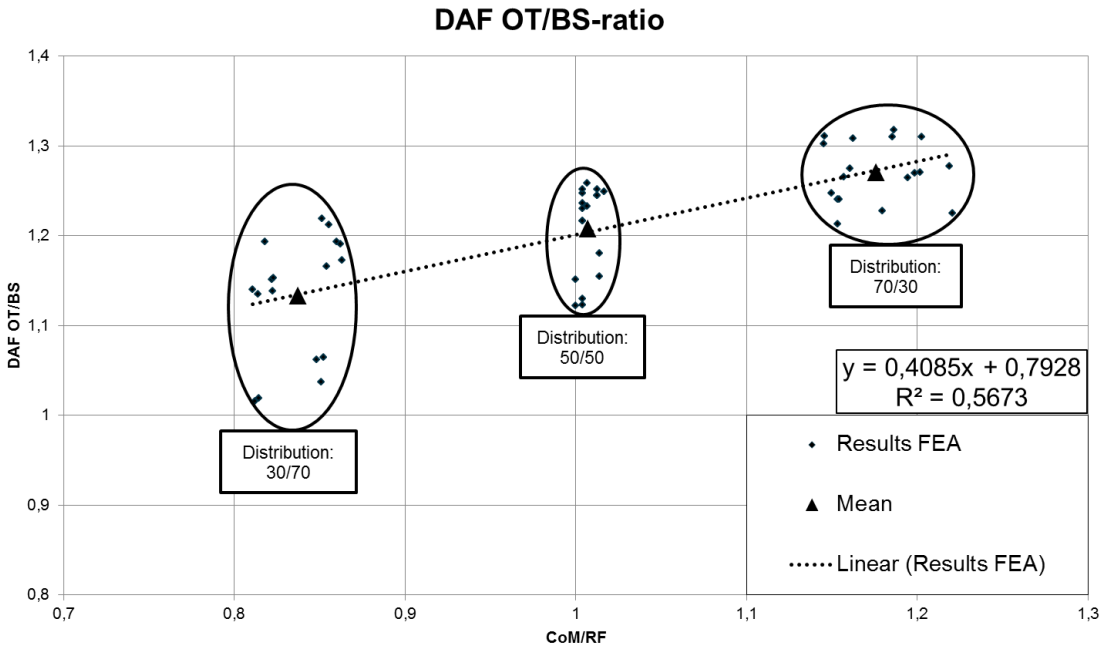

Figure 7-9 Correlation between the CoM/RF-ratio and DAF OT/BS-ratio.

As illustrated in Figure 7-9 a correlation exists between the DAF-ratio (OT/BS) and the pipe mass distribution even though the scatter is superficial. Mean, maximum and minimum values from Figure 7-9 is presented in Table 7-3.

Table 7-3 Mean, maximum and minimum values from Figure 7-9.

	Mean values		Maximum values		Minimum values	
Pipe mass distribution	CoM/ RF	DAF OT/BS	Model	DAF OT/BS	Model	DAF OT/BS
30/70	0.837	1.1332	48	1.219	51	1.015
50/50	1.007	1.2079	47	1.259	50	1.122
70/30	1.176	1.2710	25	1.318	16	1.214

Mass concentration higher up in the structure (70/30) results in an average increase in DAF-ratio of 27.1 % with a maximum increase for model 25 of 31.8 %. The lowest OT/BS-ratio is 1.015 (model 51) which compared to model 25 results in a variation of 0.303 from lowest to highest OT/BS-ratio. Moreover, the scatter in the OT/BS-ratio is

[5] The RF-coordinate is the coordinate of the resultant force that could substitute all blast loads resulting in the same moment at the supports.

greater for structures with the majority of the pipe mass placed in the bottom of the structure (30/70) and decreases as the CoM moves upwards.

In order to quantify the tendencies of the results, a linear regression is executed. The output from this regression is presented in Table 7-1 and is in accordance with the least square method[6] which is described in Eurocode 0 (EN1990, 2008). The coefficient of determination (R^2), quantifying the level of correspondence between the observed values and the linear approximation as a value between 0 and 1, is 0.5673. A perfect match would give a R^2 equal to 1, hence the deviation of the results from the linear regression is high. The error terms coefficient of variation (V_δ), which is the mean deviation of the results, is 0.0433.

Table 7-1 Output from least square method calculations.

Output	Value	Description
V_δ	0.0433	Error terms coefficient of variation
R^2	0.5673	Coefficient of determination (0-1)

[6] Least square method is a method of fitting a graph data so as to minimize the sum of the squares of the differences between observed values and estimated (Oxford University Press, 2010).

7.2.2.3 Aspect ratio and total mass

The AR is according to Table 7-2 influencing the stiffness of the structure with Eigen periods varying from 0.181 to 0.291. The DAF-curves however, are kept close to constant. As depicted in Figure 7-10, DAF-curves based on BS for structures with varying AR and mass are fairly constant with maximum DAFs scattering between 1.30-1.35. The same tendency, but with a greater variation is apparent for DAF-curves based on OT, where maximum DAFs scattering between 1.60-1.69.

Table 7-2 Eigen period of structures presented in Figure 7-10.

Mass	AR	*T*
High	5/3	0.291
Low	5/3	0.266
High	5/5	0.287
Low	5/5	0.263
High	3/5	0.197
Low	3/5	0.181

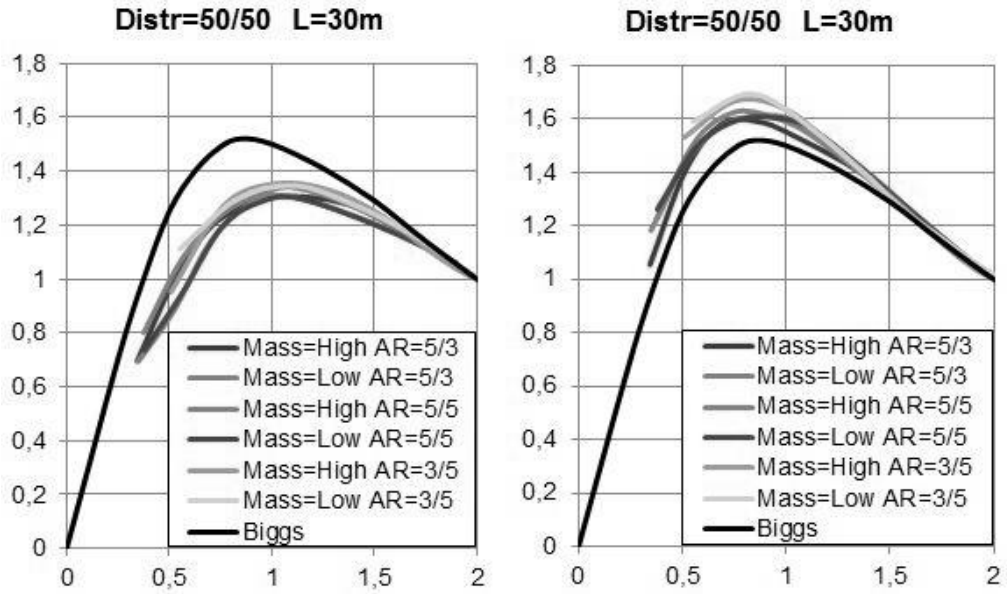

Figure 7-10 DAF-curves based on BS (left) and OT (right) for varying AR, constant mass distribution and length.

As for the pipe mass distribution, sensitivity analyses are executed for both these parameters as well. By evaluating the trend lines depicted in Figure 7-11 the effect of AR and total mass are further highlighted. The results related to AR are presented in Figure 7-11 and show a tendency of higher DAFs based on BS for structures with a 5/3-AR. For OT on the other hand, an AR of 3/5 seems to result in lower DAFs. With regard to the total mass it does not appear to be any correlation between increased mass and maximum DAFs as presented in Figure 7-12. Overall, the total mass and AR reveal no obvious tendency associated with the maximum DAFs even though a small tendency related to the AR is noticeable.

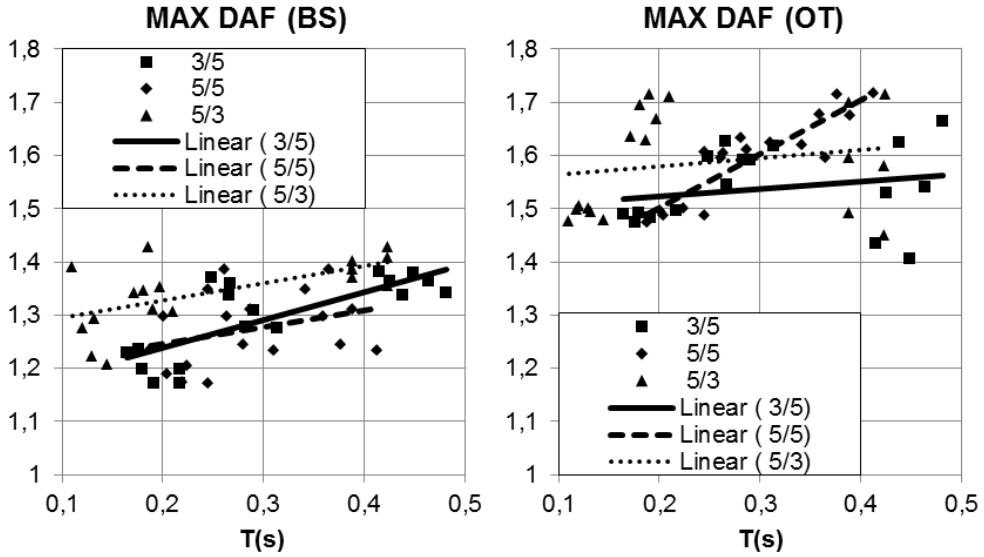

Figure 7-11 Sensitivity analysis of maximum DAF related to AR.

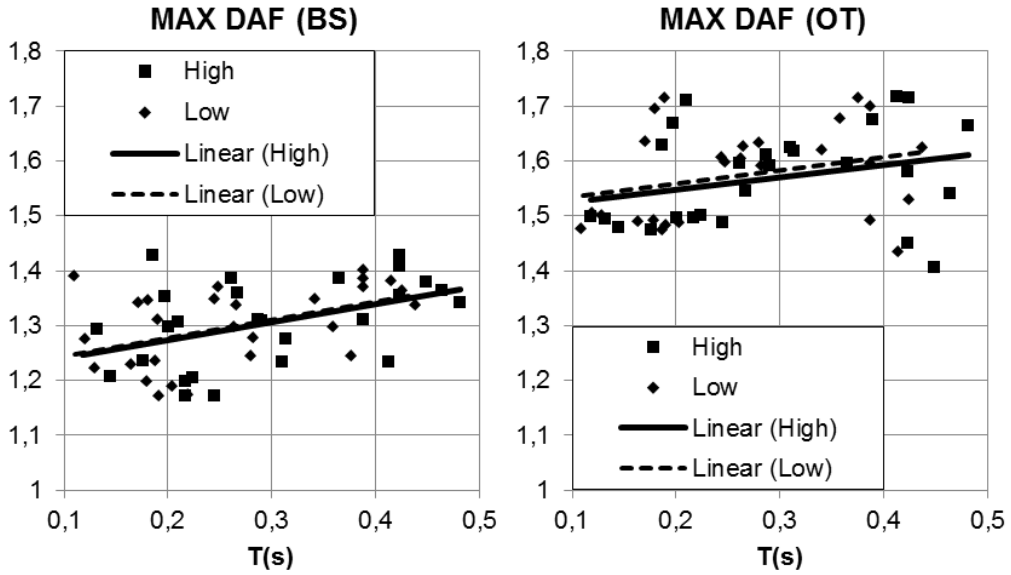

Figure 7-12 Sensitivity analysis of maximum DAF related to total mass.

7.2.2.4 Length

Increasing the length of a structure generally resulted in a slower vibrating structure, i.e. increased Eigen period (*T*). For this reason it is interesting to investigate whether there exists a relationship between the structural length and the maximum DAF. For this investigation the best method of presenting the results is by a sensitivity study. In Figure 7-13 the results are presented and from that conclusions related to length can be drawn. Firstly, it is obvious that the shorter structures result in a reduced *T* which is in accordance with the generalisation stated previously. For BS there is a correlation between increased length and higher DAF. The same is also observed for DAFs based on OT for structures with short length (10 m), where DAFs are kept fairly constant at 1.5. For the longer structures though, there is no obvious correlation.

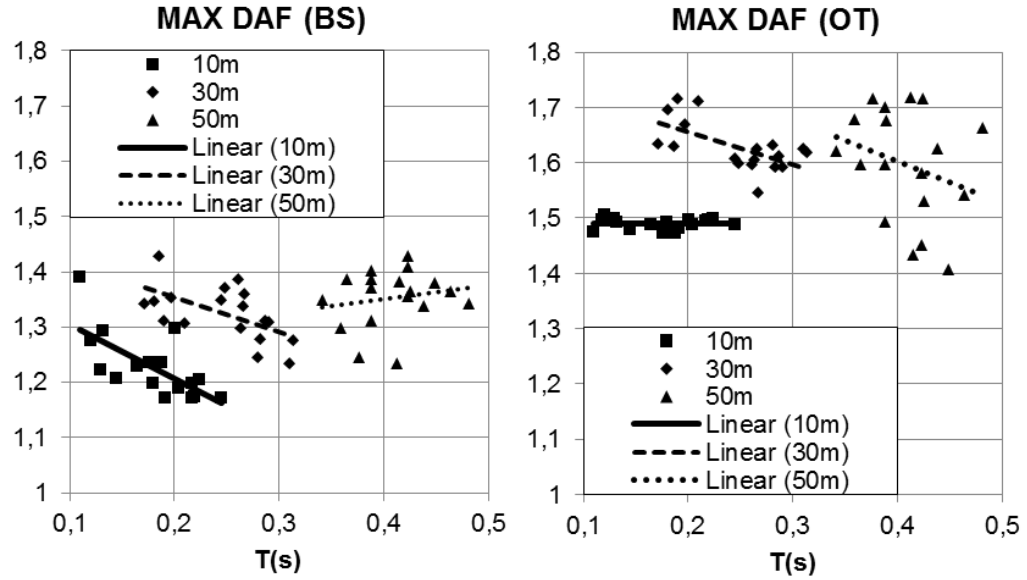

Figure 7-13 Sensitivity analysis of maximum DAF related to length.

7.2.2.5 Eigen periods

The Eigen period of a structure is dependent of the relationship between the structures stiffness and mass as described in Chapter 2 Section 2.1.3. In terms of structural dynamics, Eigen period is an important parameter and for that reason the Eigen period is presumed to have influence on the DAF-curves. However, as depicted in Figure 7-14 and Figure 7-15, there is no observable correlation between structures with similar Eigen periods and their DAF-curves. For DAFs based on BS the difference between the highest and lowest maximum DAFs is 10.7 % for structures with $T \approx 0.190$ s and for structures with $T \approx 0.375$ s it is 8.4 %.

For DAF calculated based on OT the same lack of correlation is observed. Even though the curves for model 14 and 24 ($T \approx 0.190$ s**)** are almost identical, the difference compared to model 46 is 14.0 %, which is slightly higher than the results for BS. For structures with $T \approx 0.375$ s the difference is as high as 16.0 %.

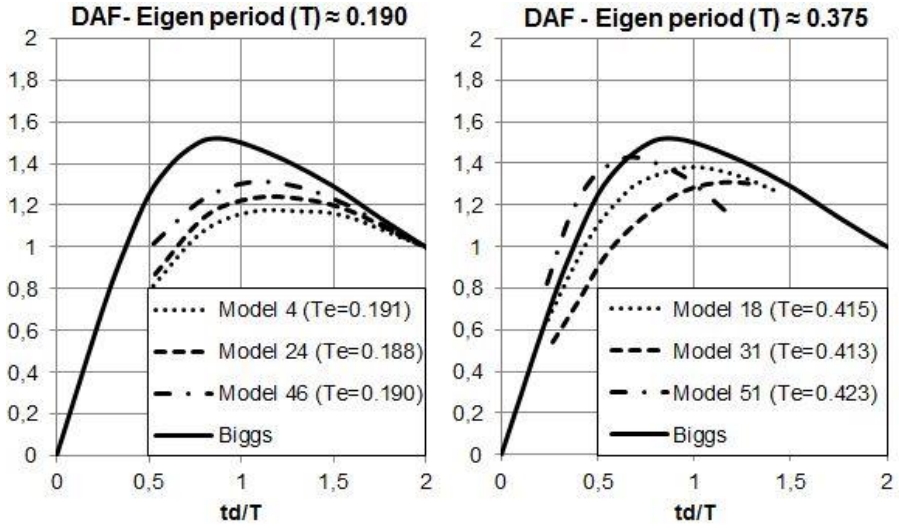

Figure 7-14 Comparison of structures with similar Eigen periods based on BS.

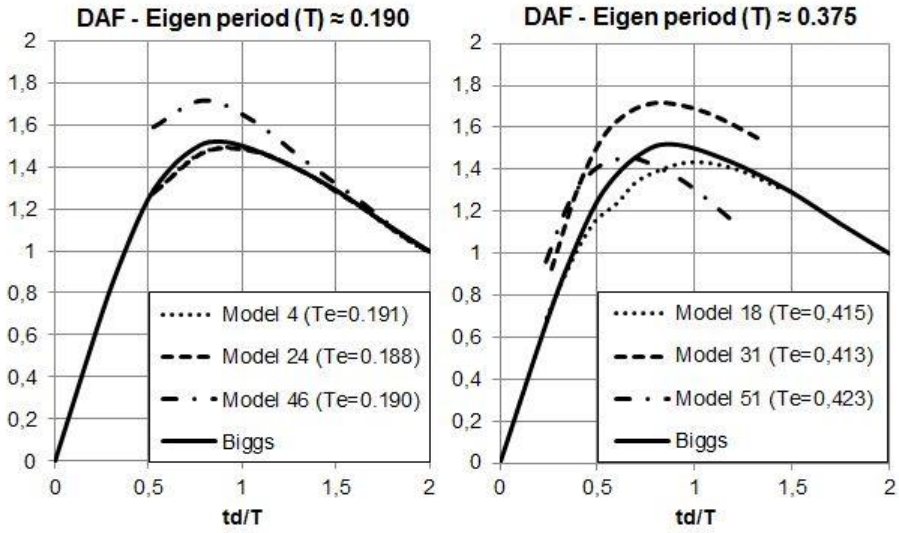

Figure 7-15 Comparison of structures with similar Eigen periods based on OT.

7.2.2.6 Extreme values

The maximum DAF-values for all the 54 structures are presented in Figure 7-16. The extreme values are marked in the figure and the properties of these structures are given in Table 7-3.

Table 7-3 Properties of structures with extreme values.

Model	*T* (s)	AR	*L* (m)	Total mass	Distribution	DAF (BS)	DAF (OT)
1	0.217	3/5	10	High	70/30	1.170	1.50
15	0.449	3/5	50	High	30/70	1.379	1.41
31	0.413	5/5	50	High	70/30	1.233	1.72
45	0.186	5/3	30	High	30/70	1.428	1.63

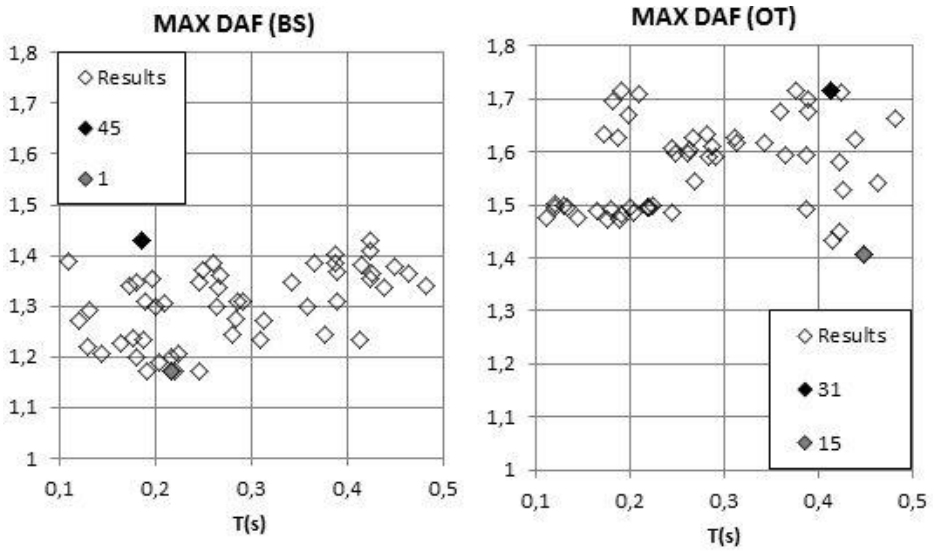

Figure 7-16 Maximum DAF for the 54 structures analysed in the parametric study.

7.2.3 Discussion of parametric study

A discussion of the results from the parametric study is presented in the following chapter. The main focus in the discussion is kept to the difference between DAFs based on BS and OT as well as the variation achieved with varied pipe mass distributions. Recommendations of further work are presented in Chapter 9.

7.2.3.1 Determination of DAF

From the results presented in the previous chapter it is clear that DAF-curves based on OT are higher than DAF-curves based on BS. The reason for this is not determined but the presented results show a relation to the pipe mass distribution on the structure. Throughout the work with the report this difference has been discussed with experts on the subject who have also experienced similar tendencies in their work on the subject without being able to state a clear reason for this behaviour. Also, a great amount of effort has been expended finding relevant scientific literature on the subject without success. Based on this, further studies on the subject are recommended with the aim of gaining better understanding of the differences between DAFs based on BS and OT.

7.2.3.2 Evaluation of parameters

Mass distribution

The difference in DAFs based on BS and OT indicates that the relationship between the location of RF and CoM is decisive for the maximum DAF as well as the shape of the DAF-curve. As presented in Section 7.2.2.2, a high CoM relative to RF results in a reduced DAF-curve for BS. For OT however, the opposite is apparent and CoM placed higher up in the structure is resulting in an increased DAF-curve.

Compared to the other studied parameters, mass distribution is a parameter which realistically would be possible to change without interfering considerably with the global geometry of the structure. Therefore, it is assumed possible to add or reduce weight in a specific location of the structure if this would decrease the DAF. However, as stated above, the location of the CoM relative to RF is affecting the DAF in different matters when studying BS and OT. Hence, to determine whether additional weight added to the top of the structure increase or decrease the DAF is not straight forward.

In the design process it would be possible to limit the mass distribution resulting in a reduced DAF compared to the DAF achieved when all three distributions are allowed. To exemplify this, two alternatives are given:

Alternative 1:

> Only pipe mass distribution 70/30 is allowed, resulting in the lowest possible maximum DAF for BS of 1.37. For the same mass distribution however, the maximum DAF based on OT is 1.72.

Alternative 2:

> Pipe mass distribution is limited to 30/70, resulting in a DAF based on OT of 1.63 and a corresponding DAF based on BS of 1.43.

Adapting alternative 2 would result in the following design procedure:

1. Apply the static load multiplied by a DAF of 1.63 to the structure.
2. Design members and connections with regard to the applied load.
3. Design the uplifting force in the base plates connecting the pipe rack to the concrete columns.
4. Reduce the base shear in the base plates by 1-(1.43/1.63) = 12 % to account for the lower DAF based on BS.

In addition to limiting the mass distribution according to alternative 2, it is worth mention that combining a low mass distribution with a low or high Eigen period, the maximum DAF based on OT can significantly be decreased. This is illustrated in Figure 7-8 in Section 7.2.2.

Whether alternative 1 or 2 will result in reduced costs for a project such as NYX in total is difficult to estimate without performing quantitative calculations. However, it is recommended to investigate further whether other parameters can be adjusted to achieve an additional reduction in DAF based on OT before introducing an economical aspect.

Aspect ratio and total mass

According to the results presented, AR as well as the total mass of the structures does not have a clear correlation with the shape of the DAF-curves. The results are clear and no further discussion is needed.

Length

When evaluating the length in relation to DAFs based on BS, the tendency is that longer structures results in higher DAFs. The same trend is not valid for DAFs based on OT where some of the longest models (50 m) reveal relatively low DAFs. However, when investigating these models further they appear to have a mass distribution of 30/70. This finding corresponds well to what was previously determined regarding mass distribution and DAF based on OT and at the same time conclude that the maximum DAFs can be slightly reduced if the length is limited.

Eigen periods

When the hypothesis regarding the outcome of the parametric study was outlined, Eigen period was brought up as an essential parameter because of its importance in structural dynamics. The mass distribution is influencing the DAF quite significantly, even though the Eigen period is kept close to constant and therefore no clear correlation between the Eigen period and the shape of the DAF-curve seems to exist. This outcome is helpful in understanding how important a systemized method of study is to fulfil the aim of the study. By establishing a hypothesis, performing studies and presenting the results in a proper way, conclusions are able to be drawn and well-argued assumptions can be established based on the achieved results.

7.3 MDOF-systems represented by the Biggs-curve

The DAF-curve from Biggs (ref. Figure 1-3) is based on a SDOF-system while the curves presented in this report are based on analyses of MDOF-systems. One of the aims of the thesis is to investigate if the DAF-curve in Biggs is representative for a MDOF-system.

When studying the DAF-curves based on BS and OT in Chapter 6 Section 6.1.1 it is found that the curves based on BS lay below or close to the Biggs-curve. Hence, when looking at only DAFs based on BS it seems conservative to assume that the Biggs-curve is valid for a MDOF-system. However, when studying the DAF-curves based on OT which generally lay above the Biggs-curve, designing structures based on the Biggs-curve tends to be non-conservative, i.e. the curve is not representative for a MDOF-system. The reason for this is not clear, but there is an obvious correlation between the variation in DAF values based on BS and OT and the ratio between the location of CoM and RF as discussed in Section 7.2.3.1. Even though Figure 7-9 show a scatter in the results for the structures with a pipe mass distribution low in the structure, there exists a tendency that this mass distribution results in the lowest DAF OT/BS-ratio (1.0-1.22).

These contradictions in behaviour imply that further studies should be performed on this topic before concrete conclusions can be drawn. A further discussion of this matter is presented together with the other further work recommendations in Chapter 9.

8 Conclusions

Based on the results from the performed studies and discussed outcomes the following conclusions are drawn:

- To adapt a DAF of 1.5 for all structures in NYX is non-conservative.
- The Biggs-curve is not representative for all MDOF-systems.
- The dynamic behaviour can be modified by changing the centre of mass of the structure.
- The lowest maximum DAF is 1.63 and is achieved for structures with the lower pipe mass distribution.
- The structural length influences the DAF-curves, with the lowest DAFs found for the shortest lengths.
- In general, aspect ratio, total mass and Eigen period do not have any noticeable correlation with the DAF-curves.
- The dynamic behaviour of steel pipe racks exposed to explosion loads should be studied further based on the outcome of this report.

9 Further work

This master's thesis could become the start of a comprehensive investigation of the dynamic response of pipe rack steel structures due to explosion loads. During the studies, additional aspects moving away from the objective of this thesis have been raised. Presented in this chapter is a summary of recommended topics that the authors of this report believe would be of interest to anyone undertaking further study.

Parametric ratios

As stated in the conclusions, the aspect ratios, total mass and Eigen periods do not show any correlation with the shape of the DAF-curves. The mass distribution however does show a correlation. Also the length seems to have influence on the DAF-curve although not in the same extent as the mass distribution. Especially for the DAFs based on BS, a correlation between the length and the mass distribution is present. Based on this it could be interesting to study the length and mass distribution further, aiming to establish a relationship between these parameters and the dynamic behaviour.

Biggs DAF-curve and DAFs based on overturning moments

One of the questions at issue in this report was whether the DAF-curve from Biggs (ref. Figure 1-3) based on a SDOF-system, is representative for a MDOF-system. As discussed in Chapter 7 Section 0, this seems to hold for the DAFs based on BS but not for OT. The DAF-curves based on BS lay beneath and not far from the DAF-curve from Biggs, while the curves based on OT most often are above it. Hence, there is a tendency that the DAFs based on OT differ from the Biggs-curve and therefore the curve is not valid for all MDOF-systems. This tendency and the reason for this should be studied further aiming to clearly state when and why the Biggs-curve can and cannot be used for MDOF-systems.

Probabilistic values

In the performed analyses the blast duration has been varied from 50-500 ms to generate the DAF-curves presented in Chapter 6 and 7. No consideration has been taken to the probability of these durations. Hence, an interesting topic to study is the structural behaviour of pipe racks exposed to explosion loads with blast durations of a limited duration range. In that matter, Eigen periods could be found for which the DAF has its lowest maximum value. Structures could then be designed to meet these limits resulting in a less conservative design.

Another aspect related to probability is the magnitude of the drag peak pressure (ΔPd). From DAL Spec. this value is given a maximum value of 0.1 bar. As mentioned in the simplification in modelling (Chapter 4 Section 4.4) it is conservative to assume the same peak pressure for all variation of duration. Hence, to decrease this conservatism, attention should be given to the potential of reducing the peak pressure when durations other than 300 ms are analysed.

Added mass or structural steel

As discussed in Chapter 7 Section 7.2.3.2 a pipe mass distribution of 30/70, i.e. with 30 % of the pipes on the top frame of the structure and 70 % on the bottom frame, results in the lowest DAFs based on OT. When the position of the centre of mass is shifted due to a change in pipe mass distribution, the DAFs based on BS are still lower than OT. Hence, DAFs based on OT is determining in design. For this reason it is profitable to design structures that are heavier in the bottom. To achieve this, the pipes could be arranged so that the centre of mass is located in the lower part of the structure. In practice however, the arrangement of the pipes is difficult to change as it depends on other neighbouring structures as well as the overall layout of the facility. Two other options for obtaining a heavier structure in the bottom is also conceivable; designing the structure to have larger or heavier profiles in the bottom or by adding masses to the lower frame in terms of lumped masses. In order to determine the most profitable option, a comparison should be performed where the following arguments should be taken into account and evaluated to find the most cost efficient design.

- Which option gives the lowest dynamic amplification, i.e. the lowest maximum DAF, and thereby the least conservative design?
- Which alternative is the most cost efficient with regard to material costs and working hours for design?
- What alternative is the most time efficient and thus cost efficient, with regard to the construction process?

Categorization of structures

Further variation of structures in addition to the ones chosen in the parametric study of this report should be evaluated. The structures should be chosen so that they can be categorized by maximum DAFs, i.e. find structures with specific lengths and mass distributions that have the same maximum DAFs. By achieving this, structures could be categorized by e.g. length/mass distribution, and maximum DAFs could be related to these categories.

Shielding and turbulence effects

The reliability on drag calculations in terms of including the effects of shielding and turbulence is treated in Chapter 2 Section 2.3.2.3, concluding that additional research should be done with regard to this topic. This implies that either CFD-analyses of different pipe rack steel structures or full-scale experiments should be performed. In NYX, a shielding factor of 0.5 is used for the pipe racks, i.e. the second (back) frame is loaded by 50 % of the load compared to the first frame. The effect of turbulence is not considered which is incorrect as the turbulence accelerates the blast and counteracts with the shielding effect. Overall, this could result in non-conservative designs of the structures. For this reason, design procedures in future projects should be evaluated and include the effect of turbulence.

DAFs based on BS and DAFs based on OT

As there exist obvious differences between the DAF-curves based on BS and OT, it is probable that the dynamic amplification in the base plate could be decreased. This could be executed by utilizing a DAF based on OT in the design of the structures, while the DAF can be reduced according to the OT/BS-ratio in design of the base plates. This theory is discussed in Chapter 7 Section 7.2.2.1, but should be verified by analysing base plates with regard to BS and OT.

Principal component analysis

In future studies, it could be preferable to use principle component analysis (PCA) to interpret results from parametric studies. The central idea of PCA is to reduce the dimensionality of a data set consisting of a large number of interrelated variables, while retaining as much as possible of the variation present in the data set (Jolliffe, 2002). This is achieved by transforming the variables to a new set of variables, the principal components, which are uncorrelated, and which are ordered so that the first few retain most of the variation present in all of the original variables. By adapting PCA, results can be visualized in two or three dimensional plots in order to illustrate patterns.

As an example, PCA can be adopted in order to find patterns between the DAF(OT)/DAF(BS)-ratio, aspect ratio and the CoM/RF-ratio. The PCA can result in a three dimensional plot illustrating the relationship between the parameters and ratios.

10 Summary

The aim of this thesis was to gain better knowledge regarding the dynamic behaviour of pipe rack steel structures exposed to explosion loads. In addition to this, two questions were formulated to further state the aim:

- Can the DAF be decreased below its maximum value of 1.5 by influencing certain parameters?
- Is the DAF-curve from Biggs (ref. Figure 1-3) which is based on a SDOF-system, representative for MDOF-systems?

In order to answer these questions, FE-analyses of three pipe rack structures on NYX were performed. Before analysing the structures, the interaction between blast load and structure was studied in order to apply the correct loads including effects from both shielding and turbulence. The pipe racks were selected due to their rather large variation in geometry and mass properties in order to find tendencies in the results.

In Abaqus/CAE a representative but simplified 3D wire based FE-model was created neglecting both joints and eccentricities. For the three models, analyses of both the static and dynamic behaviour were performed in order to calculate DAFs. DAF is a factor quantifying the dynamic amplification of the static loads so that a static analysis is sufficient to design the structure. By varying the blast duration, DAF-curves were plotted against the ratio of blast duration and Eigen period for the structures. The results of the analyses showed divergence between the curves indicating that some of the parameters were affecting the dynamic behaviour of the pipe racks. Also a clear difference between DAF-curves based on base shear (BS) and curves based on overturning moments (OT) was apparent. There was however no clear pattern indicating which parameters affected the shape and magnitude of the DAF-curves. Based on these results it was concluded that a parametric study was required in order to sort out which, how and why the different parameters influence the DAF-curves.

The results from this parametric study revealed two interesting findings. Firstly, a maximum DAF of 1.5, which is utilized by AKSO for the structures in NYX, is not valid for all structures. Secondly, the same difference between BS and OT revealed in the analyses of the NYX structures was apparent in the parametric study. Additionally, some of the parameters were showing a distinct correlation to the magnitudes of the DAF-curves. From the chosen parameters, the pipe mass distribution was the parameter with the most significant influence on the DAF-curves. For DAFs based on BS for structures with the centre of mass moved upwards, i.e. a pipe mass concentration high in the structure, a reduction was clear. This implies that an increase in mass e.g. by adding additional weight in the top of the structure can reduce the maximum DAF. However, adding mass and moving the centre of mass upwards is not exclusively positive with regards to the dynamic behaviour. DAFs based on OT showed an increased maximum DAF for structures with a high centre of mass. In addition, the lowest possible maximum DAF was calculated to 1.64 and was achieved by excluding two of the pipe mass distributions, only allowing structures with the pipe mass concentrated in the lower part of the structure.

To conclude the outcomes of the study, pipe rack steel structures should be designed by multiplying the static loads with a DAF based on OT to account for the dynamic behaviour. For design of base plates a reduction relative to the difference in DAF based on OT and BS can be accounted for. With regard to if the DAF-curve from Biggs (ref.

Figure 1-3) based on a SDOF-system is representative for MDOF-systems, the results are contradictory. DAF-curves based on BS are below or close to the Biggs-curve while the DAF-curves based on OT are both below and above it. Based on this it can be concluded that the dynamic amplification of structural details influenced by BS can be designed based on the Biggs-curve while details mainly influenced by OT cannot.

After four months of analyses and calculations, the authors of this report welcome others to continue studying the dynamic behaviour of pipe rack steel structures exposed to explosion loads in order to gain further knowledge. This report and the conclusions drawn will form a good basis for these studies even though several aspects are not investigated. More detailed recommendations of further work are presented in Chapter 9.

11 References

Allaby, M., 2013. *A Dictionary of Geology and Earth Sciences.* 4th red. : Oxford University Press.

ASCE, 2010. *Design of Blast-resistant Buildings in Petrochemical Facilities,* Virginia: ASCE American Society of Civil Engineers.

Atkins, T. & Escudier, M., 2013. *A Dictionary of Mechanical Engineering.* u.o.:Oxford University Press.

Baker, W. o.a., 1983. *Explosion Hazards and Evaluation.* New York: Elsevier Scientific Publishing Company.

Biggs, J. M., 1964. *Introduction to structural dynamics.* u.o.:McGraw-Hill. Inc..

Bjerketvedt, D., Bakke, J. R. & van Wingerden, K., 1990. Gas Explosion Handbook. *Gas Safety Programme 1990*.

Bjørkhaug, M., 1986. *Flame acceleration in obstructed radial geometries,* Bergen, Norway: Christian Michelsen Institue.

Bro, R. & Smilde, A. K., 2014. Principle component analysis. *Analytical Methods,* Issue 6, pp. 2812-2831.

Craig, R. R. J., 2006. *Fundamentals of Structural Dynamics.* 2 red. Hoboken, New Jersey: John Wiley & Sons Inc.

Daintith, J., 2008. *A Dictionary of Chemistry.* 6th red. u.o.:Oxford University Press.

DNV, 2010. *Recommendes Practice DNV-RP-C205 Environmental Conditions and Environmental Loads,* u.o.: Det Norske Veritas AS.

DNV, 2013. *Recommended Practice DNV-RP-C208 Determination of Structural Capacity by Non-linear FE analysis Methods,* Oslo: DNV.

EN1990, 2008. *Euro Code 0, Basis of structural design, Part D8.2.2.* u.o.:European Committee for Standardisation.

Hjertager, B. H., 1984. Professor. *Journal of Hazardous Materials,* 9(3), pp. 315-346.

Jolliffe, I. T., 2002. *Principle Component Analysis.* 2nd red. Secaucus, NJ: Springer.

Liu, X., Levitan, M. & Nikitopoulos, D., 2008. Wind tunnel tests for mean drag and lift coefficients on multiple circular cylinders arranged in-line. *Journal of Wind Engineering and Industrial Aerodynamics 96,* pp. 831-839.

Mannan, S., 2014. *Lees' Process Safety Essentials.* 1st red. Waltham: Elsevier Inc..

Merx, I. W., 1992. *Methods for the determination of possible damage to people and objects resulting from release of hazardous materials - Chapter 2 The consequences of explosion effects on structures,* Voorburg: The Hague: Directorate-General of Labour of the Ministry of Social Affairs and Employment. III..

Oxford University Press, 2010. *Oxford Dictionary,* Oxford: Oxford University Press.

Paz, M., 1987. *Structural Dynamics - Theory and Computation (1985).* 2nd red. New Dehli: S.K Jain CBS Publishers & Distributors in arrangement with Van Nostrand Reinhold Company Inc..

Prud'homme, S., Legeron, F., Laneville, A. & Tran, M. K., 2013. Wind forces on single and shielded angle members in lattice structures. *Journal of Wind Engineering and Industrial Aerodynamics*, p. 9.

Shell, 2014. *www.shell.no.* [Online]
Available at: http://www.shell.no/products-services/ep/ormenlange/en.html
[Accessed 07 04 2014].

Yandzio, E. & Gough, M., 1999. *Protection of buildings against explosions.* U.K.: The Steel Construction Institute.

Yavari, A., 2010. [Online]
Available at: http://imechanica.org/node/8437
[Accessed 11 March 2014].

Appendix A – Blast load calculations

This appendix includes Excel sheets with calculations of the blast loads on pipes and RHSs.

Table A-I Blast load on pipes according to DNV-RP-C205 (DNV, 2010).Constants are found in Table A-II and A-III.

Pipe						**Structure**						
Structure	Piping class	Position	Diameter (b) [m]	t [m]	Area (S) [m2]	srack [m]	smin [m]	l [m]	b [m]	φ	A [m2]	Ac [m2]
R56BV01	CC2	BOT	8,89E-02	3,05E-03	0,09	4,20	0,17	43,95	5	0,52	219,75	114,27
R56BV01	CC2	BOT	1,14E-01	3,05E-03	0,11	4,20	0,17	43,95	5	0,52	219,75	114,27
R56BV01	CD1	BOT	6,03E-02	2,77E-03	0,06	4,20	0,17	43,95	5	0,52	219,75	114,27
R56BV01	CD1	BOT	6,03E-02	2,77E-03	0,06	4,20	0,17	43,95	5	0,52	219,75	114,27
R56BV01	HA4	BOT	1,68E-01	2,20E-02	0,17	4,20	0,17	43,95	5	0,52	219,75	114,27
R56BV01	HD4	BOT	6,03E-02	5,50E-03	0,06	4,20	0,17	43,95	5	0,52	219,75	114,27
R56BV01	KC2	BOT	1,14E-01	1,75E-02	0,11	4,20	0,17	43,95	5	0,52	219,75	114,27
R56BV01	HA4	MID	1,68E-01	2,20E-02	0,17	4,20	0,35	43,95	5	0,52	219,75	114,27
R56BV01	HA4	MID	2,73E-01	2,86E-02	0,27	4,20	0,35	43,95	5	0,52	219,75	114,27
R56BV01	HA4	MID	7,62E-01	6,50E-02	0,76	4,20	0,35	43,95	5	0,52	219,75	114,27
R56BV01	HC1	MID	1,14E-01	1,11E-02	0,11	4,20	0,35	43,95	5	0,52	219,75	114,27
R56BV01	HD3	MID	6,03E-02	5,50E-03	0,06	4,20	0,35	43,95	5	0,52	219,75	114,27

Shape								Blast Load						
Structure	q = ΔPd	ρair	ν	v	Re=b*v/ν	Flow range	Ce	Fw,SOL	α	a	β	η	Fw,SHI	Fw,SHI/ Fw,SOL
	[N]	[kg/m3]	[m/s]	[m/s]				[N/m]					[N/m]	[%]
R56BV01	1,00E+04	1,25	1,50E-05	126	7,5,E+05	Supercritical	0,80	370	24	0,60	0,31	0,95	351	95 %
R56BV01	1,00E+04	1,25	1,50E-05	126	9,6,E+05	Supercritical	0,80	475	24	0,60	0,31	0,95	452	95 %
R56BV01	1,00E+04	1,25	1,50E-05	126	5,1,E+05	Supercritical	0,80	251	24	0,60	0,31	0,95	238	95 %
R56BV01	1,00E+04	1,25	1,50E-05	126	5,1,E+05	Supercritical	0,80	251	24	0,60	0,31	0,95	238	95 %
R56BV01	1,00E+04	1,25	1,50E-05	126	1,4,E+06	Supercritical	0,80	700	24	0,60	0,31	0,95	665	95 %
R56BV01	1,00E+04	1,25	1,50E-05	126	5,1,E+05	Supercritical	0,80	251	24	0,60	0,31	0,95	238	95 %
R56BV01	1,00E+04	1,25	1,50E-05	126	9,6,E+05	Supercritical	0,80	475	24	0,60	0,31	0,95	452	95 %
R56BV01	1,00E+04	1,25	1,50E-05	126	1,4,E+06	Supercritical	0,80	700	12	0,60	0,31	0,95	665	95 %
R56BV01	1,00E+04	1,25	1,50E-05	126	2,3,E+06	Supercritical	0,80	1136	12	0,60	0,31	0,95	1079	95 %
R56BV01	1,00E+04	1,25	1,50E-05	126	6,4,E+06	Supercritical	0,80	3170	12	0,60	0,31	0,95	3011	95 %
R56BV01	1,00E+04	1,25	1,50E-05	126	9,6,E+05	Supercritical	0,80	475	12	0,60	0,31	0,95	452	95 %

R56BV01	1,00E+04	1,25	1,50E-05	126	5,1,E+05	Supercritical	0,80	251	12	0,60	0,31	0,95	238	95 %

Table A-II Shielding factor η from (DNV, 2010)*).*

β / α	*0.1*	*0.2*	*0.3*	*0.4*	*0.5*	*0.6*	*0.7*	*0.8*
< 1.0	1.0	0.96	0.90	0.80	0.68	0.54	0.44	0.37
2.0	1.0	0.97	0.91	0.82	0.71	0.58	0.49	0.43
3.0	1.0	0.97	0.92	0.84	0.74	0.63	0.54	0.48
4.0	1.0	0.98	0.93	0.86	0.77	0.67	0.59	0.54
5.0	1.0	0.98	0.94	0.88	0.80	0.71	0.64	0.60
> 6.0	1.0	0.99	0.95	0.90	0.83	0.75	0.69	0.66

The *spacing ratio* α is the distance, centre to centre, of the frames, beams or girders divided by the least overall dimension of the frame, beam or girder measured at right angles to the direction of the wind. For triangular or rectangular framed structures diagonal to the wind, the spacing ratio should be calculated from the mean distance between the frames in the direction of the wind.

The *aerodynamic solidity ratio* is defined by $\beta = \phi a$ where

ϕ = solidity ratio, see 5.3.2

a = constant

= 1.6 for flat-sided members

= 1.2 for circular sections in subcritical range and for flat-sided members in conjunction with such circular sections

= 0.6 for circular sections in the supercritical range and for flat-sided members in conjunction with such circular sections.

Table A-III Effective shape coefficient C_e from (DNV, 2010) .

Solidity ratio ϕ	*Effective shape coefficient Ce*		
	Flat-side members	*Circular sections*	
		$Re < 4.2 \times 10^5$	$Re \geq 4.2 \times 10^5$
0.10	1.9	1.2	0.7
0.20	1.8	1.2	0.8
0.30	1.7	1.2	0.8
0.40	1.7	1.1	0.8
0.50	1.6	1.1	0.8
0.75	1.6	1.5	1.4
1.00	2.0	2.0	2.0

Table A-IV Blast load on RHSs according to DNV-RP-C205 (DNV, 2010).Constants are found in Table A-II and A-III.

Pipe					**Structure**						
Structure	Piping class	Position	Width (d)	Height (b)	srack	smin	l	b	φ	A	Ac
			[m]	[m]	[m]	[m]	[m]	[m]		[m2]	[m2]
L56BV01	300x300x12,5	Bottom	0,3	0,3	4,2	0,17	15,27	3,45	0,52	52,68	27,39
L56BV01	300x300x12,5	Top	0,3	0,3	4,2	0,35	15,27	3,45	0,52	52,68	27,39
L56BV01	300x300x12,5	Vertical	0,3	0,3	4,2	4,20	15,27	3,45	0,52	52,68	27,39
L56BV01	300x300x30	Vertical	0,3	0,3	4,2	4,20	15,27	3,45	0,52	52,68	27,39
L56BV01	300x200x12,5	Diagonal	0,3	0,2	4,2	4,20	15,27	3,45	0,52	52,68	27,39

Shape					**Blast Load**						
Structure	q=ΔPd	ρair	ν	Ce	Fw,SOL	α	a	β	η	Fw,SHI	Fw,SHI/Fw,SOL
	[N]	[kg/m3]	[m/s]		[N/m]					[N/m]	
L56BV01	10000	1,25	126	1,6	2496	24	0,6	0,31	1	2371	95 %
L56BV01	10000	1,25	126	1,6	2496	1	1,6	0,83	0,4	924	37 %
L56BV01	10000	1,25	126	1,6	2496	1	1,6	0,83	0,4	924	37 %
L56BV01	10000	1,25	126	1,6	2496	1	1,6	0,83	0,4	924	37 %
L56BV01	10000	1,25	126	1,6	1664	1	1,6	0,83	0,4	616	37 %

Appendix B – Point blast loads

Table B-I Point blast loads in the position of pipe supports.

Structure	Piping class	Name Abaqus	Position	Diameter (b) [m]	t [m]	S (Area) [m2/m]	Fw [N/m]	Fw,SHI [N/m]	L [m]	Fw,point [N]
R56BV01	HA4	4A	MID-1	2,73E-01	2,86E-02	0,27		1079	3,9	4209
		4B	MID-2	2,73E-01	2,86E-02	0,27		1079	3,6	3885
		4C	MID-3	2,73E-01	2,86E-02	0,27		1079	3,6	3885
		4D	MID-4	2,73E-01	2,86E-02	0,27		1079	2,4	2590
R56BV01	HC1	3A	MID-1	1,14E-01	1,11E-02	0,11		452	3,9	1762
		3B	MID-2	1,14E-01	1,11E-02	0,11		452	3,6	1626
		3C	MID-3	1,14E-01	1,11E-02	0,11		452	3,6	1626
		3D	MID-4	1,14E-01	1,11E-02	0,11		452	8,1	3659
R56BV01	HA4	2A	MID-1	1,68E-01	2,20E-02	0,17		665	3,9	2594
		2B	MID-2	1,68E-01	2,20E-02	0,17		665	3,6	2394
		2C	MID-3	1,68E-01	2,20E-02	0,17		665	3,6	2394
		2D	MID-4	1,68E-01	2,20E-02	0,17		665	3,6	2394
R56BV01	HA4	1A	MID-1	7,62E-01	6,50E-02	0,76	3170		12,2	38515
		1B	MID-2	7,62E-01	6,50E-02	0,76	3170		13,2	41684
									Σ	1,13E+05

Appendix C – A study of Δt effects

In this appendix, the effect of assuming $\Delta t = 0$ is evaluated by comparing the results from analyses with $\Delta t = 0$ and $\Delta t > 0$.

Firstly, the theoretical velocity (v) of the blast is derived from

$$kinetic\ energy = \frac{mv^2}{2} \tag{C.1}$$

resulting in

$$v = \sqrt{\frac{2*energy}{m}} = \sqrt{\frac{2*\Delta Pd}{\rho_{air}}} \tag{C.2}$$

where ΔPd is the drag peak pressure given in DAL Spec. and ρ_{air} is the density of air. Secondly, the study is performed for one of the parametric models and Δt is calculated by dividing the width of the structure (s) by the theoretical velocity of the blast

$$t = \frac{s}{v} \tag{C.3}$$

For the chosen structure (model 26) $\Delta t = 0.040\ s$. A comparison of the peak of the DAF-curves obtained with $\Delta t = 0.040\ s$ and $\Delta t = 0$ is presented in Figure C-1. This study indicates that it is conservative to assume $\Delta t = 0$, i.e. the assumption made in the simplifications in Chapter 4 Section 4.4 is correct.

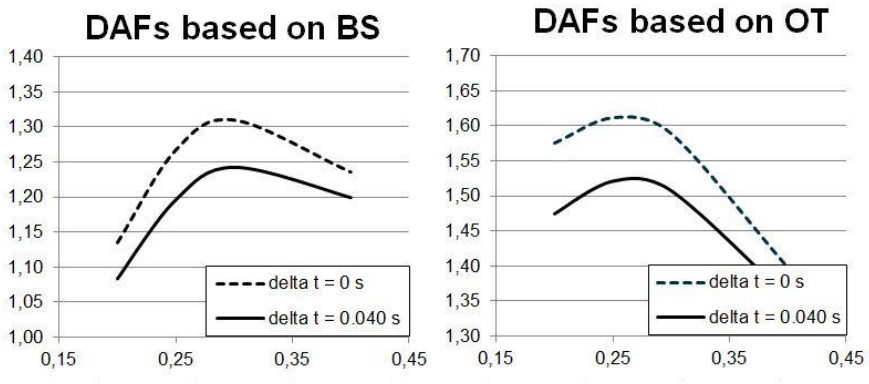

Figure C-1 Comparison of DAF-values for analyses with Δt = 0 and Δt = 0.040 s.